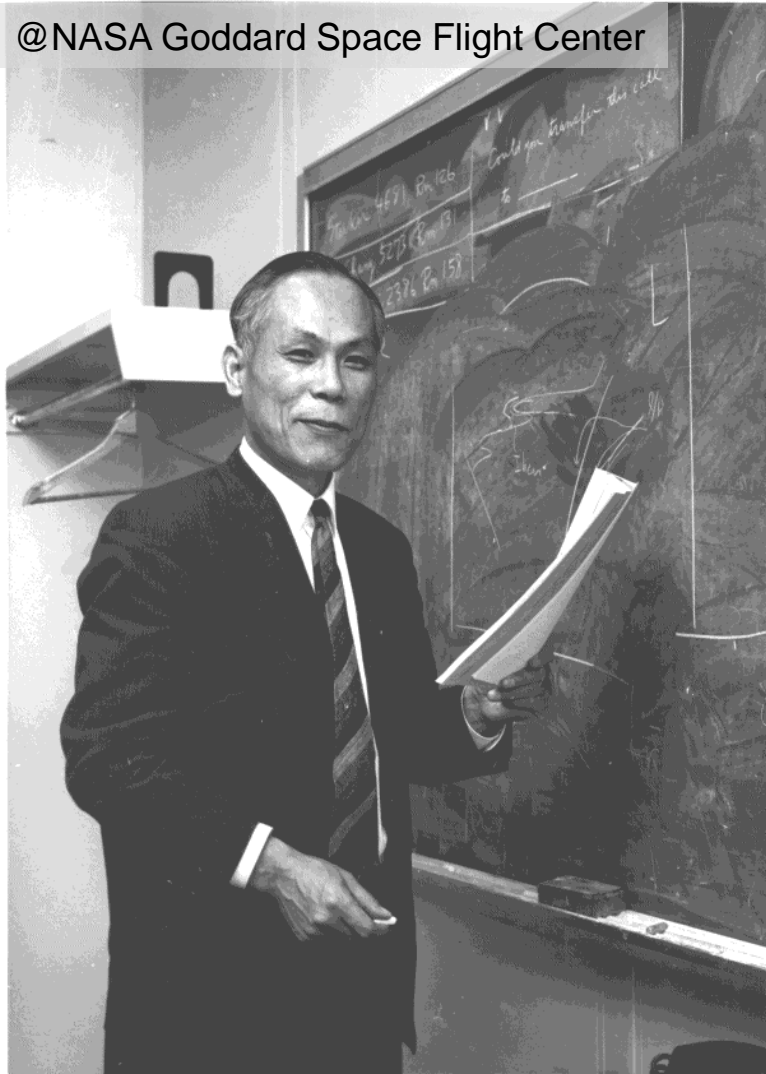


星間媒質と星形成

@NASA Goddard Space Flight Center



犬塚修一郎(名大・理・物理)

Special Thanks to

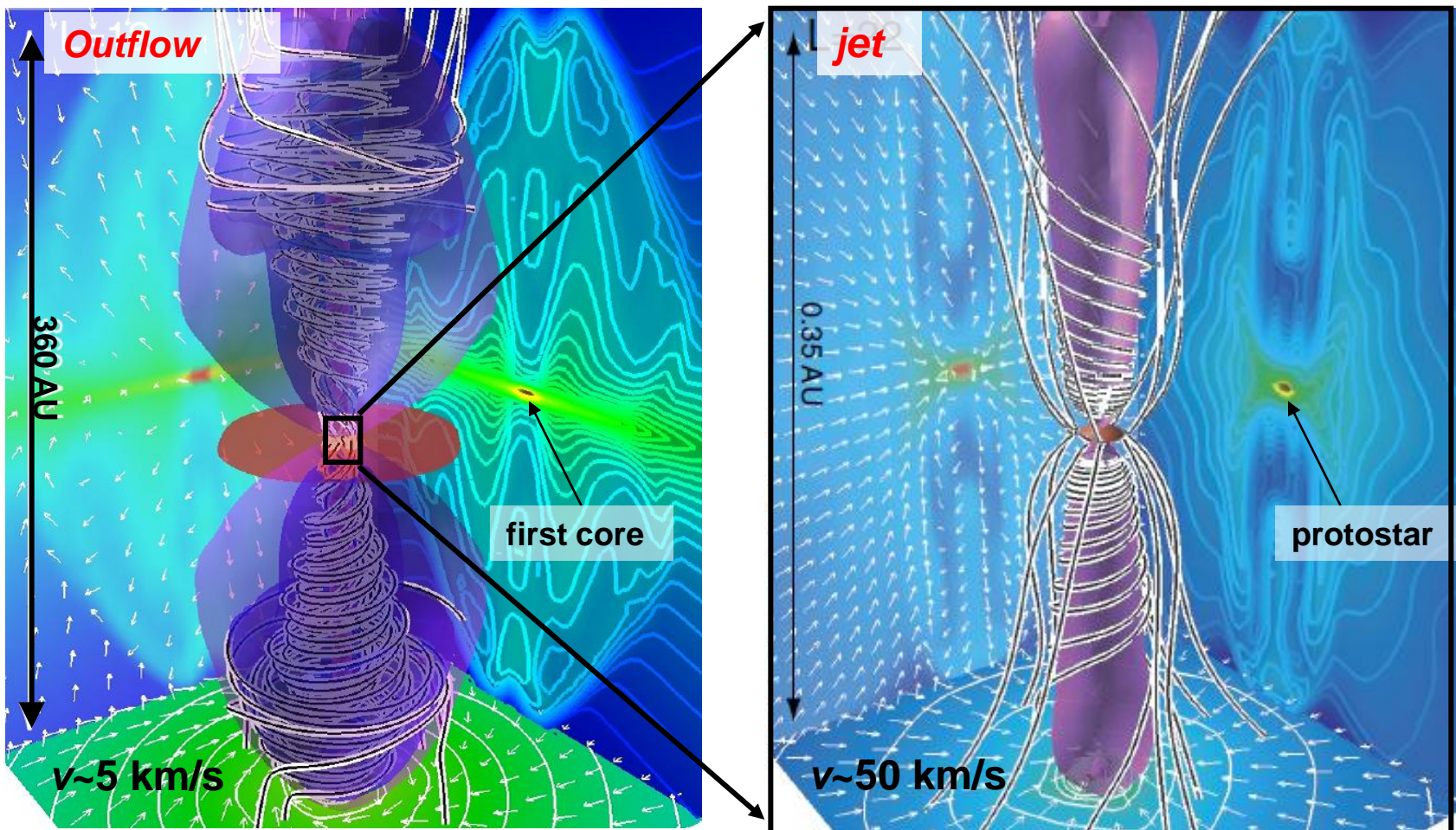
観山正見, 中野武宣, 富阪幸治, 花輪知幸, 西亮一, 中村文隆, 松本倫明, 西合一矢, 町田正博, 釣部通, 増永浩彦, 永井智哉, 大向一行, 小山洋, 細川隆史, 井上剛志, 岩崎一成, 他



中沢清教授の退官記念の研究会(2008京都)



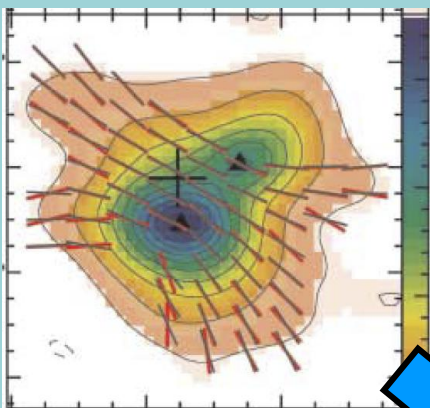
Part 1: Protostellar Collapse Phase



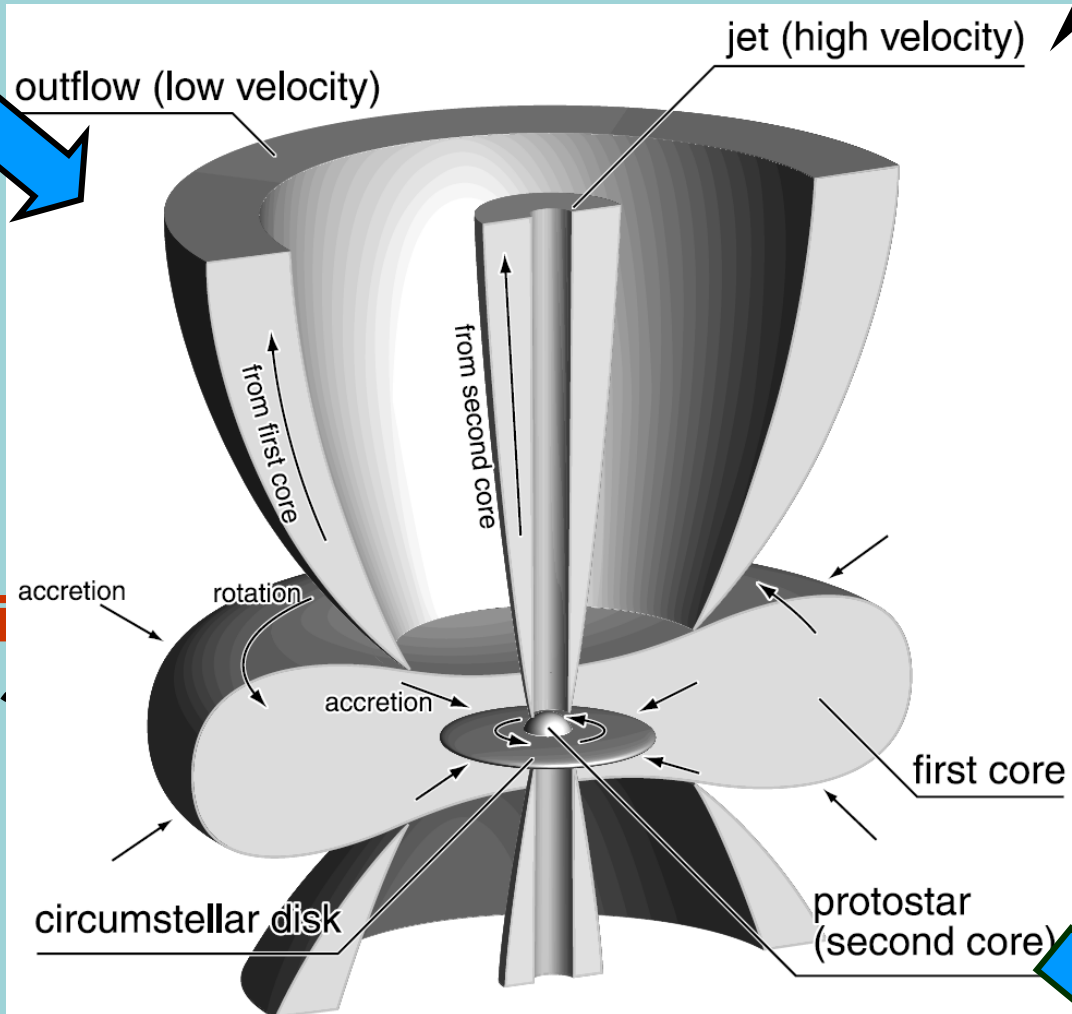
Machida et al. (2006-2009), Banerjee & Pudritz (2006), Hennebelle & Fromang (2008)

Outflows & Jets are Natural By-Products!

星形成の各段階



分子雲コア
~10⁴AU



前期段階:
ガス収縮期

後期段階:
ガス降着期

原始惑星
系円盤

~10⁶⁻⁷ yr

TTauri, MSへ

惑星形成へ



星形成の基本問題

1. 角運動量問題

原始星(Protostar):

$$h_* = \Omega_* R_*^2 \sim (10^{11}\text{cm})^2 / (10^5\text{s}) \sim 10^{17} \text{ cm}^2/\text{s}$$

分子雲コア:

$$h_{\text{core}} = \delta v_{\text{core}} R_{\text{core}} \sim 0.1\text{km/s} \times 10^{17}\text{cm} \sim 10^{21} \text{ cm}^2/\text{s}$$

$$\rightarrow h_* \sim \mathbf{10^{-4}} h_{\text{core}}$$

2. 磁束問題

原始星(Protostar): $\Phi_* \sim B_* R_*^2 \sim \text{kG} \times (10^{11}\text{cm})^2$

分子雲コア: $\Phi_{\text{core}} \sim B_{\text{core}} R_{\text{core}}^2 \sim 10\mu\text{G} \times (10^{17}\text{cm})^2$

$$\rightarrow \Phi_* \sim \mathbf{10^{-4}} \Phi_{\text{core}}$$

重力・磁気力・圧力のスケーリング

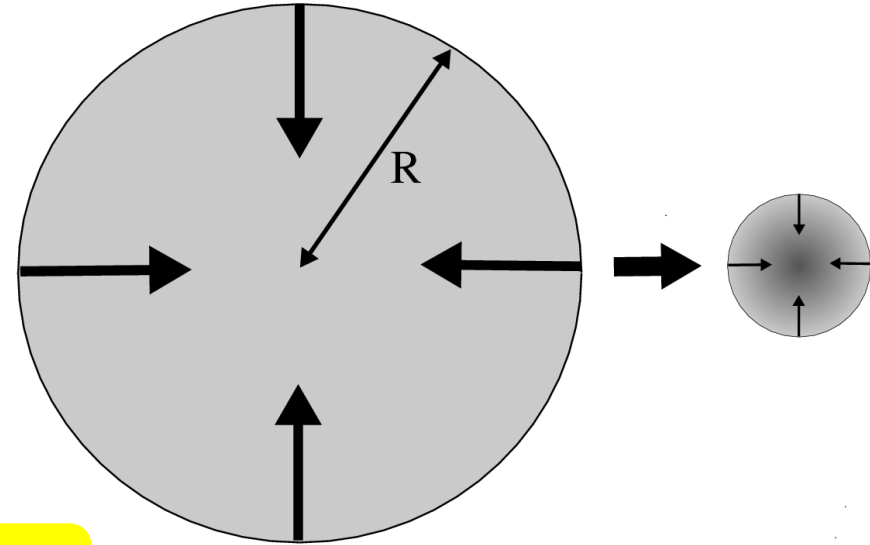
単位質量当りの力

$\rho \propto r^{-3}$, $B \propto r^{-2}$ なので,

$$\text{重力} = -\frac{GM}{r^2} \propto r^{-2}$$

$$\text{磁気圧勾配} = -\frac{1}{8\pi\rho} \frac{\partial B^2}{\partial r} \propto r^{-2}$$

$$\text{圧力勾配} = -\frac{1}{\rho} \frac{\partial P}{\partial r} \propto \frac{\rho^{\gamma-1}}{r} \propto r^{-3\gamma+2}$$



輻射冷却は本質的に重要

磁場は出番を待っている!

$\gamma < 4/3$ にならない限り重力収縮し続けない!

理想MHDでは、**磁場と重力は拮抗したまま収縮!**

重力収縮する雲の熱的進化

$1M_{\odot}$ cloud

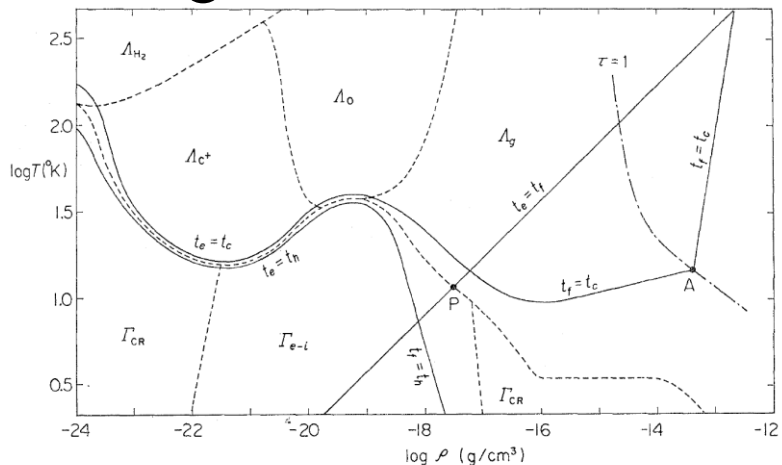


Fig. 1. The evolutionary feature of a cloud of $1M_{\odot}$ in the density-temperature diagram. Each solid curve represents the state of $t_e=t_f$, $t_e=t_c$, $t_e=t_h$, $t_f=t_c$ or $t_f=t_h$. The dashed curves divide the diagram into seven regions according to the predominant process of cooling or heating. On the boundary between the cooling region and the heating region the total of the cooling rates just counteracts that of the heating rates. On the dot-dashed curve $\tau=1$ the cloud becomes opaque to thermal radiation. If the cloud of $1M_{\odot}$ is born with a density lower than that of the critical point P, it finally expands nearly along the curve $t_e=t_h$, and returns to the interstellar medium. On the other hand the cloud which is born with a higher density finally contracts nearly along the curve $t_f=t_c$ to the point A. The evolutionary path after passing the point A is shown in Fig. 4.

$0.01M_{\odot}$ cloud

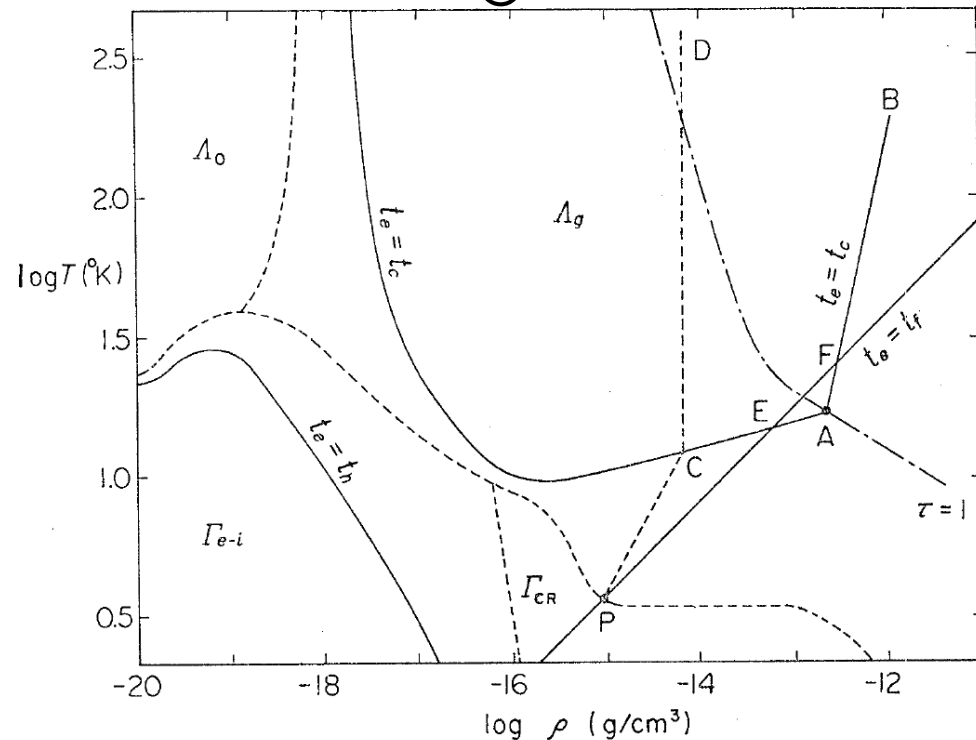


Fig. 5. The evolutionary feature of a cloud of $10^{-2}M_{\odot}$ in the density-temperature diagram. The cloud which is born in the region to the left of the dashed curve PCD is destined finally to expand along the curve $t_e=t_h$. On the other hand, the cloud which is born in a region between the curve PCD and the line $t_f=t_e$, it expands at first and settles down to the equilibrium line $t_f=t_e$. Afterwards it contracts slowly along this line emitting radiation.

自己重力的収縮の特徴：逃走的収縮

Homologous Collapse

$$P \propto \rho^\gamma, \quad C_S^2 \propto \rho^{\gamma-1}$$

$$\rho \propto 1/R^3, \quad M = \text{const.}$$

$$F_P \equiv (1/\rho)dP/dR \propto C_S^2/R$$

$$F_G \equiv GM/R^2 \propto 1/R^2$$

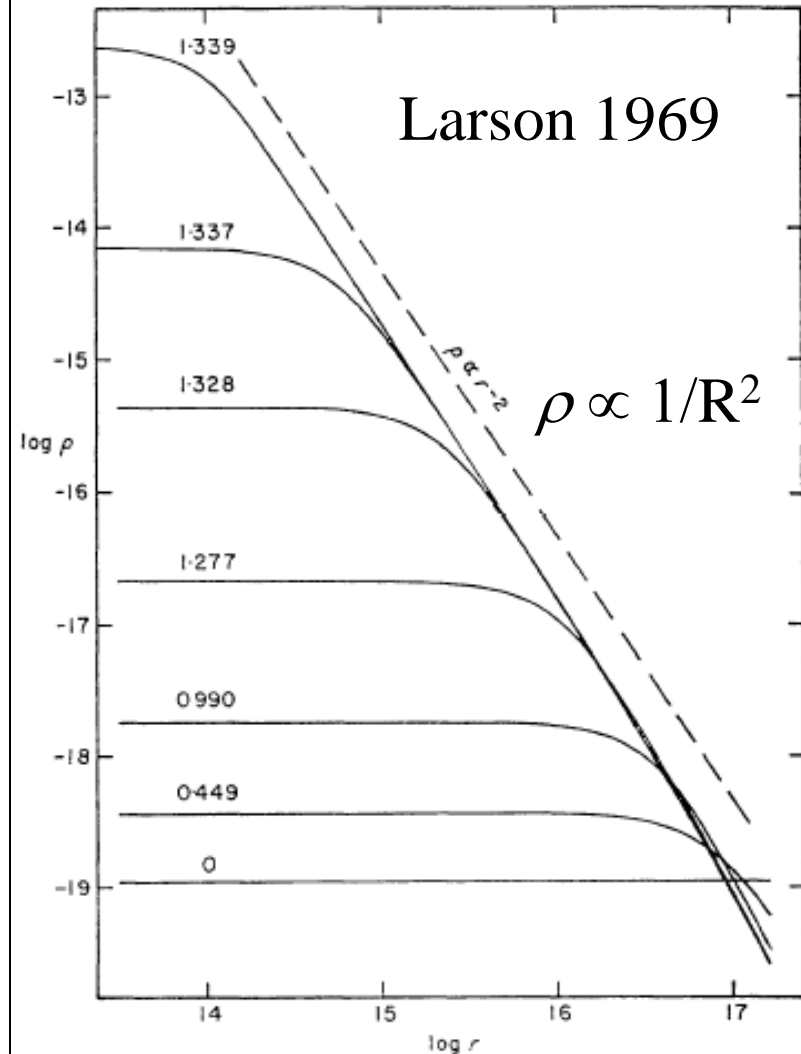
$$F_P / F_G \propto R^{-(3\gamma-4)}$$

$$\gamma_{\text{crit}} = 4/3$$

if $\gamma < 4/3 \rightarrow$ unstable

$t_{\text{ff}} \sim (G\rho)^{-0.5} \rightarrow$ run-away

Run-Away Collapse



Rotating Run-Away Collapse

Isothermal Run-Away Collapse

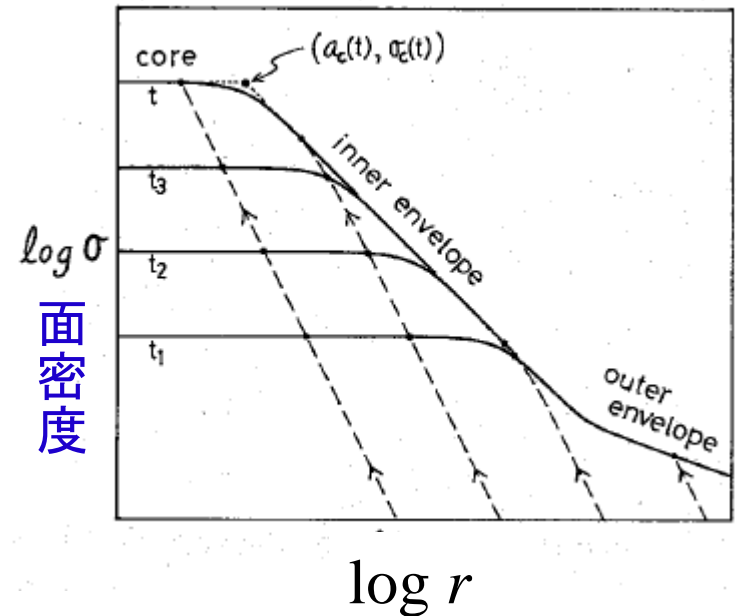
$$\Omega(t) \propto (G\rho)^{1/2}$$

$$F_C \equiv r \Omega(t)^2 \propto r \rho \propto 1/r^2$$

$$F_G \equiv \pi G \rho r z/r_c \propto r \rho \propto 1/r^2$$

$$F_C / F_G = \text{const.} < 1 \text{ @center}$$

→ Self-Similar Collapse



Narita, Miyama, Hayashi 1984

See also

Tomisaka, Basu, Matsumoto, etc.

Saigo, Matsumoto & Hanawa 2000

No Run-Away Collapse if $\gamma > 1$.

$\gamma_{\text{crit}} = 1$... isothermal

Collapse toward Protostars

Gravitational Collapse of Molecular Cloud Cores

$$(\rho \approx 10^{-19} \text{ g cm}^{-3}, \quad R \approx 10^4 \text{ AU})$$

Formation of a Protostar

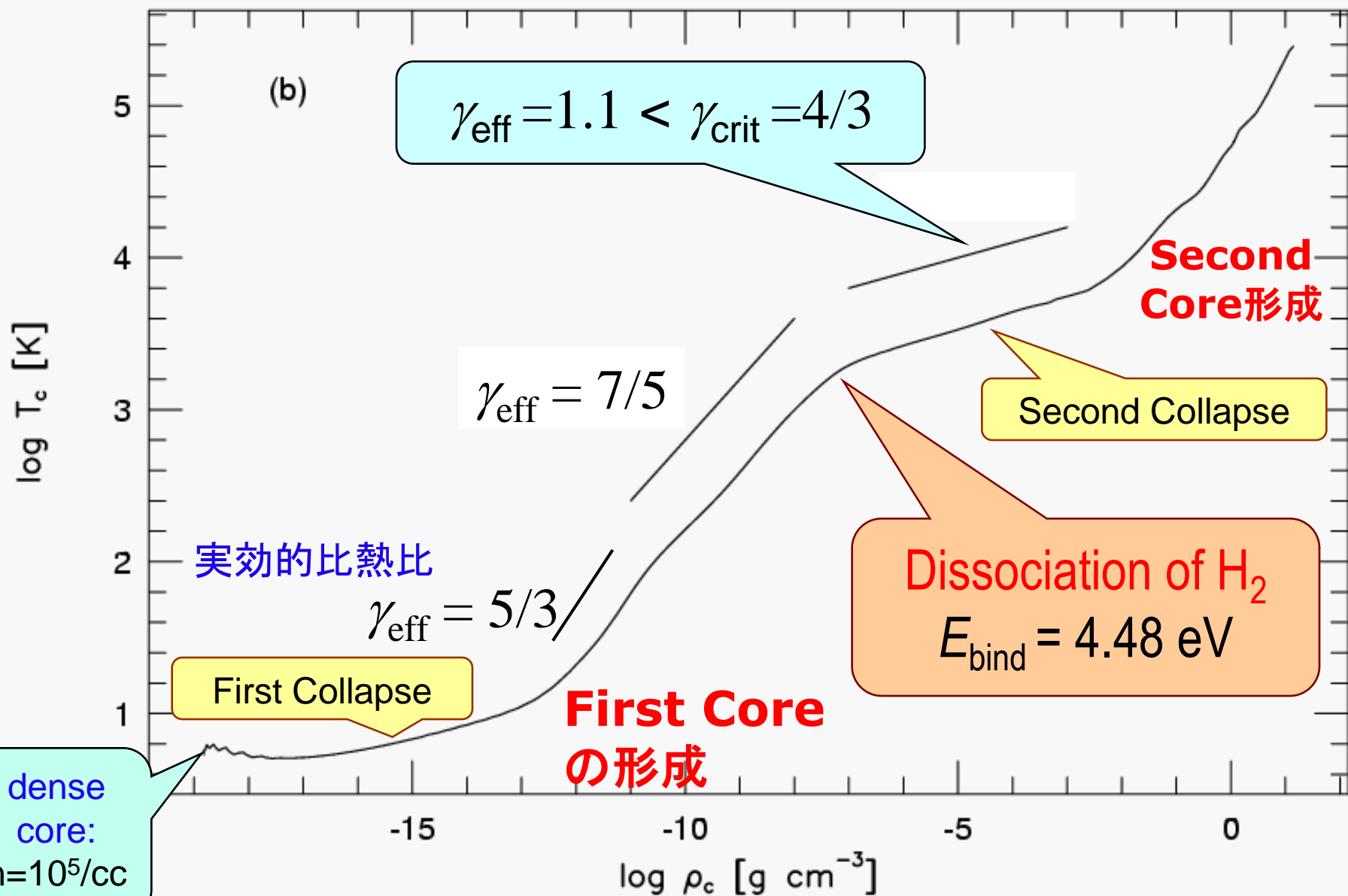
$$(\bar{\rho} \approx 1 \text{ g cm}^{-3}, \quad R \approx \text{a few } R_{\odot})$$

1D Radiation Hydrodynamical Modelling

- *Larson (1969)* diffusion approx. for radiation
- *Narita, Nakano, & Hayashi (1970)*
- *Stahler, Shu, & Taam (1980)*...quasi-static calc.
- *Winkler & Newman (1980a,b)* ...gray RHD
- *Masunaga, Miyama, & SI (1998)* **v-dependent RHD**
- *Masunaga & SI (2000)* ... **v-dependent RHD**

Disc Accretion ...2D/3D models (e.g., *Yorke et al. 2002*)

RHD: Temperature Evolution at Center



Isothermal EoS of Gas

In dense region, **gas** and **dust grains** are thermally well coupled.

Heating rate (Γ_g) and Cooling rate (Λ_g) of **Dust Grains**

$$4\pi\kappa\rho\langle I \rangle \quad \boxed{\text{initially negligible} + \Gamma_g} = 4\pi\kappa\rho\sigma_{\text{SB}}T^4 \equiv \Lambda_{\text{thin}}$$

radiative heating collisional heating by gas radiative cooling

Grains stay almost isothermal unless the gas is heated up by rapid contraction, shock, etc.

(Gaustad 1963, ApJ **138**, 1050; Hayashi 1966, ARAA **4**, 171))

Transition from Isothermal to Adiabatic Evolution

SI & Miyama 1997, ApJ **480**, 681; Masunaga & SI 1999, ApJ **510**, 822

- Gas and grains are thermally well coupled in dense region.
- Heating rate (Γ_g) and Cooling rate (Λ_g) of Grains

$$4\pi \kappa \rho I + \Gamma_g = \Lambda$$

radiative heating collisional heating radiative cooling

- Optically Thin Case ($\tau < 1$)

$$\Gamma_g \cong \frac{P}{\rho} \frac{d\rho}{dt} \approx \Lambda_{\text{thin}} = 4\pi \kappa \rho \sigma_{\text{SB}} T^4 \Rightarrow$$

$$\rho_{\text{thin}} = 4.7 \times 10^{-15} \left(\frac{\kappa}{0.01 \text{ cm}^2/\text{g}} \right)^2 \left(\frac{T}{10 \text{ K}} \right)^{10} \frac{\text{g}}{\text{cm}^3}$$

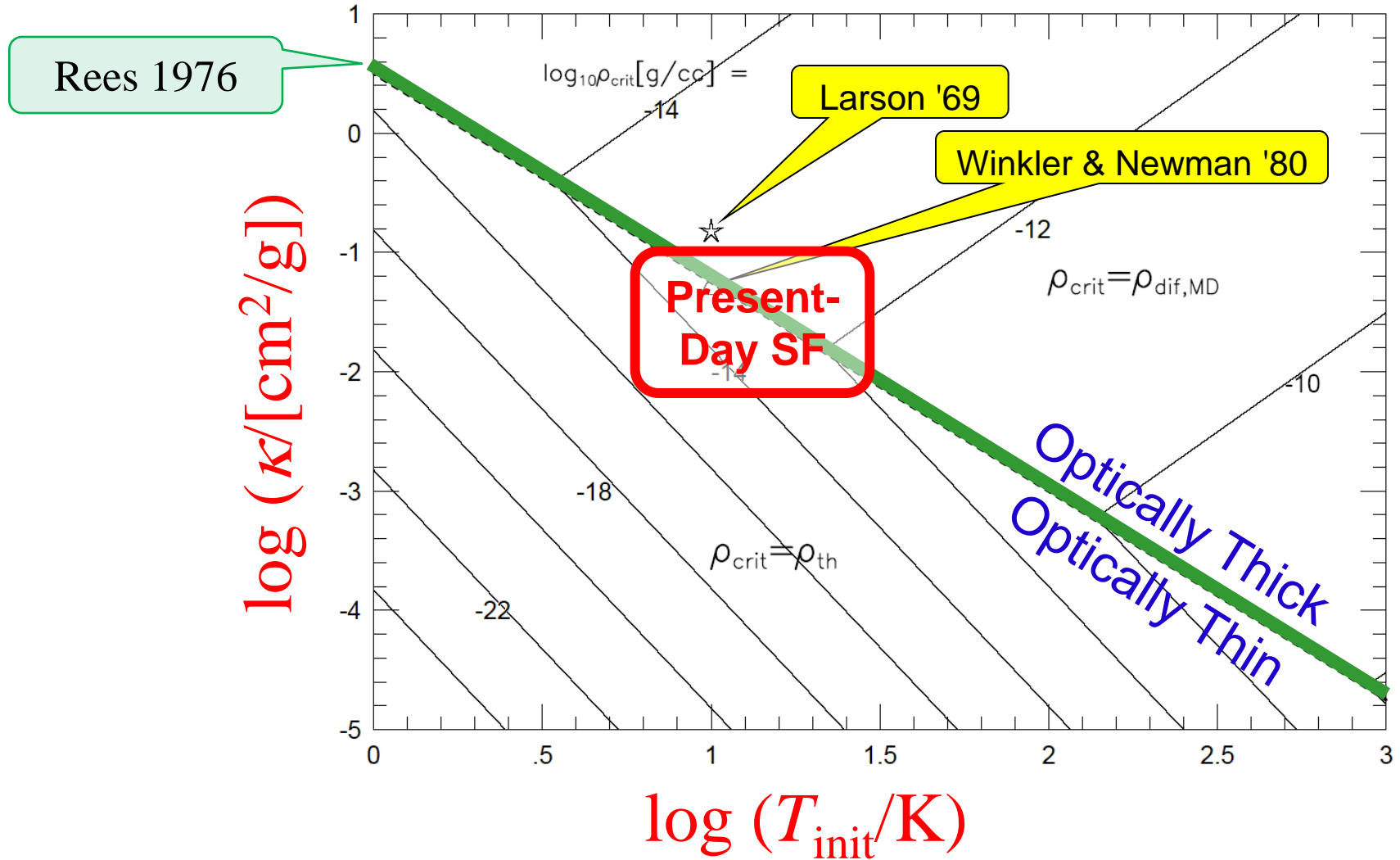
- Optically Thick Case ($\tau > 1$)

$$\Gamma_g \cong \frac{P}{\rho} \frac{d\rho}{dt} \approx \Lambda_{\text{diffusion}} \cong \frac{4\pi \kappa \rho \sigma_{\text{SB}} T^4}{\tau^2} \Rightarrow$$

$$\rho_{\text{thick}} = 4.7 \times 10^{-13} \left(\frac{\kappa}{0.01 \text{ cm}^2/\text{g}} \right)^{\frac{2}{3}} \left(\frac{T}{10 \text{ K}} \right)^{\frac{2}{3}} \frac{\text{g}}{\text{cm}^3}$$

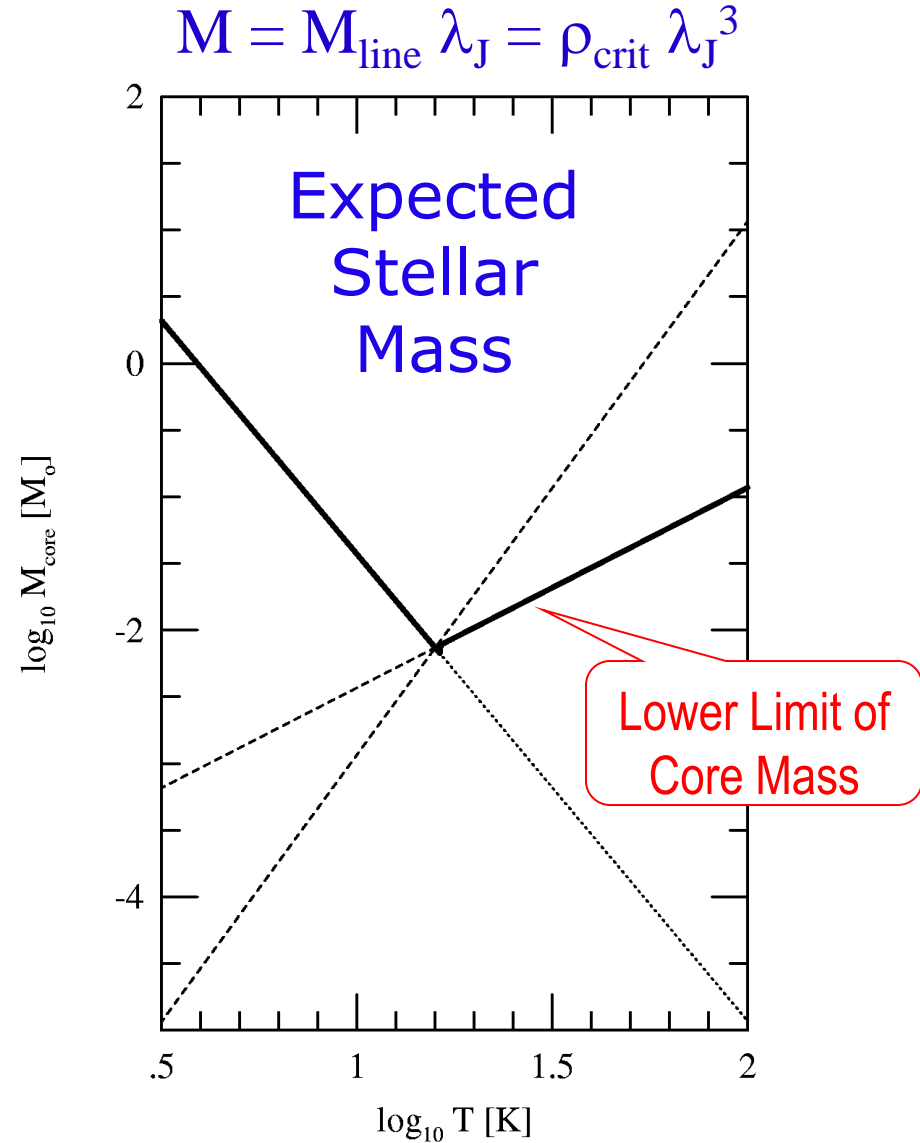
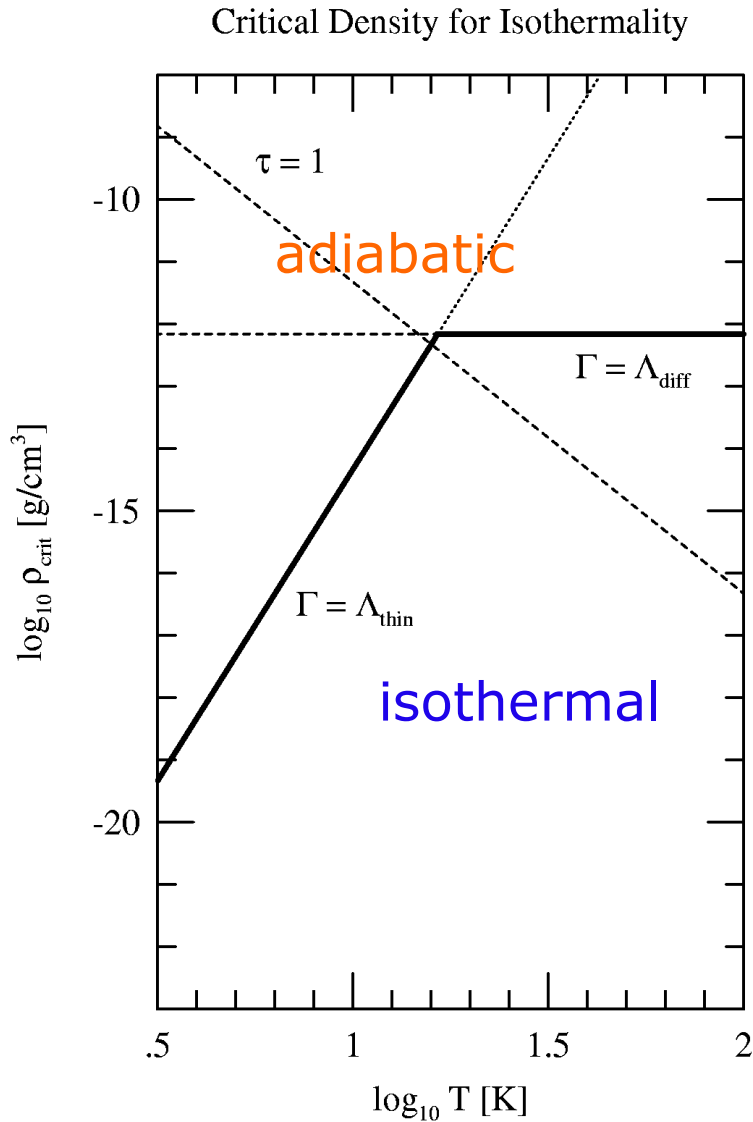
- “ $\tau \approx 1$ ” does not determine the transition condition.

温度が上がる ρ_{crit} の $\kappa-T_{\text{init}}$ 依存性

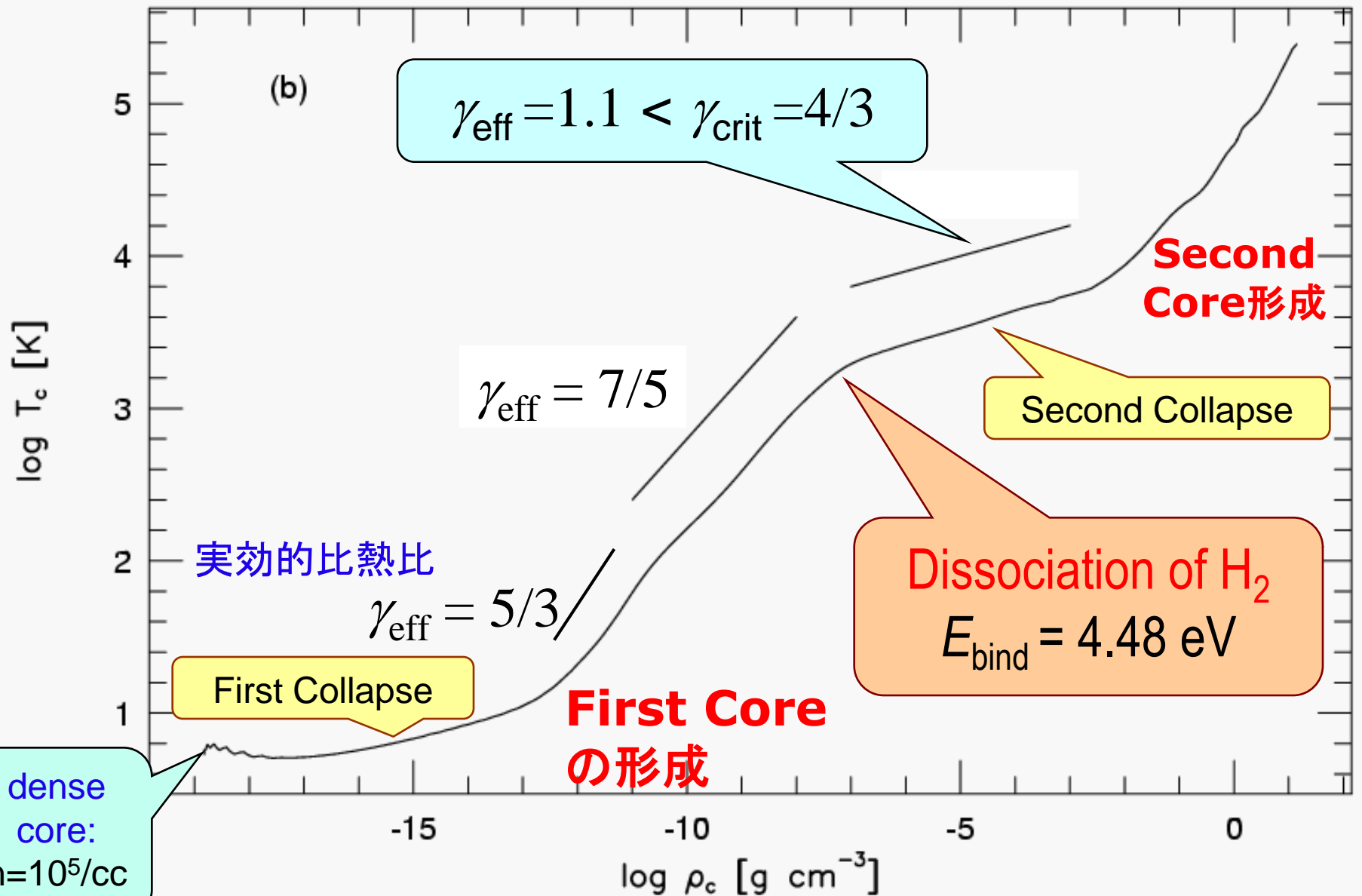


温度が上がり始める密度は雲の初期温度（環境） T_{init} と不透明度（重元素量） κ の関数である。Masunaga & SI 1999, ApJ 510, 822

Transition from Isothermal to Adiabatic Evolution



Temperature Evolution at Center



First Core形成の3Dダイナミックス

First Coreの重要性

その寿命は 10^3 yr 程度しかないが,...

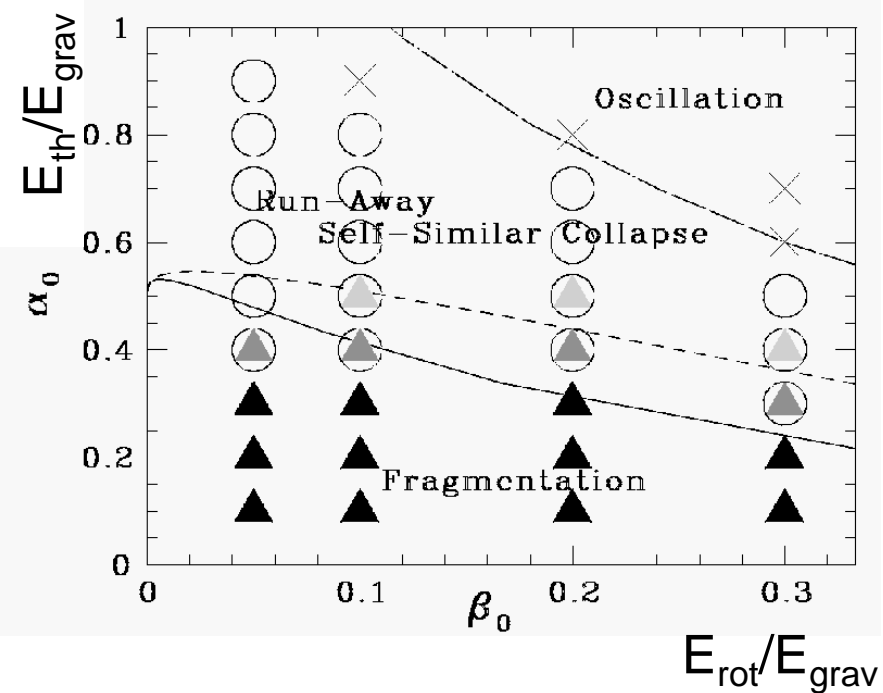
1. 円盤状構造の形成

→ 重力的分裂と連星系形成へ

2. MHD outflow の駆動

(長周期)連星の形成

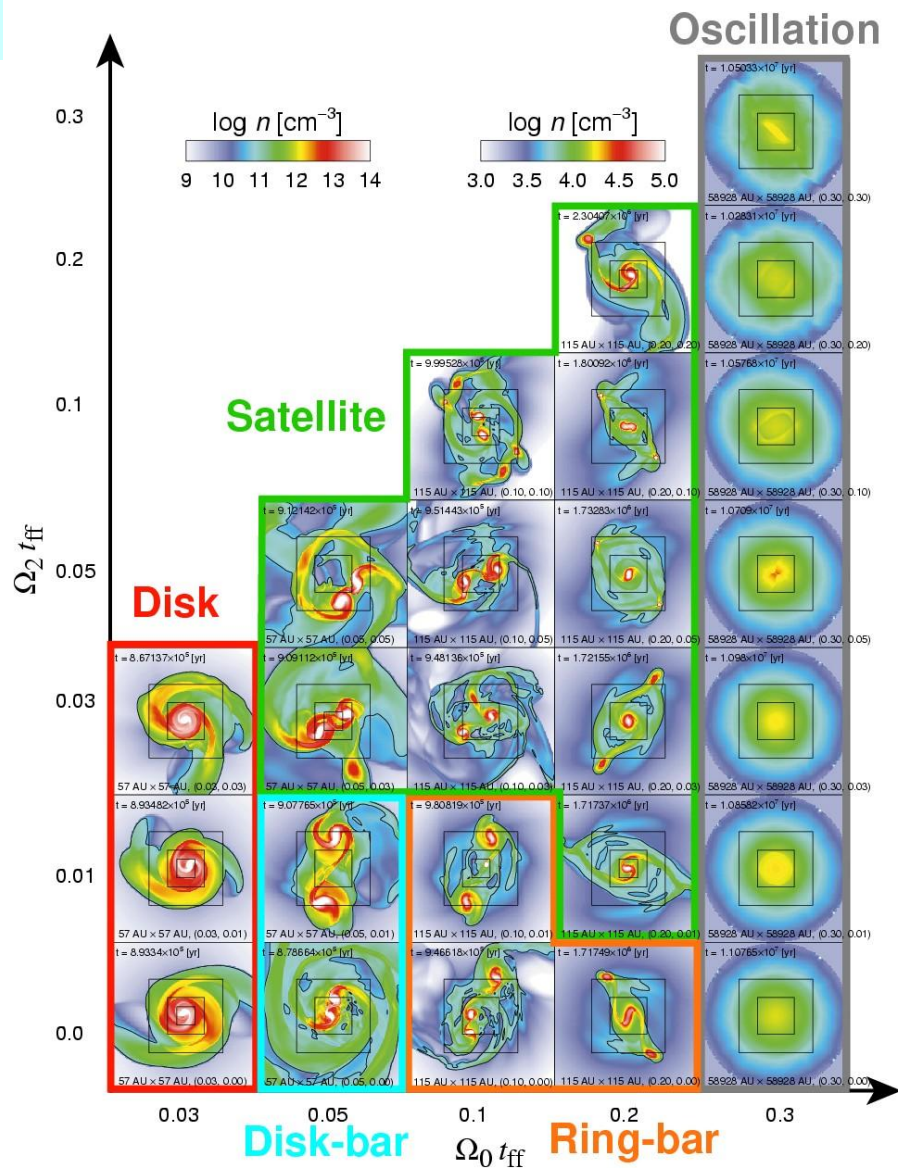
Isothermal Evolution before the Formation of First Core



Miyama, Hayashi, & Narita 1984
 Tsuribe & SI 1999, ApJ, **523**, L155;
 Tsuribe & SI 1999, ApJ **526**, 307

First Core形成前の分裂は困難

Evolution **after** Formation of First Core



Matsumoto & Hanawa (2003) ApJ **595**, 913

First Coreの分裂が重要

林先生秘伝のメモ

軸対称, flat disk (thin limit $z \rightarrow 0$) の P_s と重力

軸対称:
$$\phi(w, z) = -2\pi G \int_0^a \rho_s(w', z') w' dw' dz' - \int_0^w J_0(kw) J_0(kw') e^{-k|z-z'|} dk$$

Thin limit ($z \rightarrow 0$)

$$\phi(w, z=0) = -2\pi G \int_0^a \rho_s(w') w' dw' \int_0^w J_0(kw) J_0(kw') dk$$

$z=0$:
$$F_w = -\frac{\partial \phi}{\partial w} = -2\pi G \int_0^a \rho_s(w') w' dw' \int_0^w J_1(kw) J_0(kw') k dk$$

$$H_{10}(w, w') = \int_0^a J_1(kw) J_0(kw') k dk$$

$$= \frac{1}{w} z f\left(\frac{w'}{w}\right) = \frac{2}{\pi} \frac{E(x)}{1-x^2}$$

$$f(x) = \frac{1}{\pi} \left\{ \frac{E(x)}{1-x} + \frac{K(x)}{1+x} \right\}, \quad k^2 = \frac{4x}{(1+x)^2} = \frac{4ww'}{(w+w')^2}$$

(K, E は第1, 2種完全楕円積分)

上の逆変換:

$$2\pi G \rho_s(w) = - \int J_0(kw) J_1(kw') k dk F(w') w' dw'$$

$$\frac{Gm(w)}{w} = - \int J_1(kw) J_2(kw') k dk F(w') w' dw'$$

$$\therefore \rho_s(w) = 2\pi \int_0^w \rho_s(w') w' dw'$$

重力平均の場合

$$-F(w) \cdot w = v^2(w)$$

$$\begin{cases} 2\pi G \rho_s(w) = \int J_0(kw) J_1(kw') k dk v^2(w') dw' \\ \frac{Gm(w)}{w} = \int J_1(kw) J_2(kw') k dk v^2(w') dw' \end{cases}$$

MF: 若し Gauss の Hypergeometric function を用いた場合

$$F(\alpha, \beta; \gamma; z) = 1 + \frac{\alpha \beta}{\gamma} z + \frac{\alpha(\alpha+1)\beta(\beta+1)}{\gamma(\gamma+1) \cdot 2} z^2 + \dots$$

Surface density	mass	gravity	j-m relation (z=0)
$\rho_s(w)/\rho_0$	$m(w)/\pi a^2 \rho_0$	$-F(w)/\pi G \rho_0$	$j/j_0 \quad (j = m(w)/H)$
$(1 - \frac{w^2}{a^2})^\mu$ ($\mu > 1$)	$\frac{1}{\mu+1} \left\{ 1 - \left(1 - \frac{w^2}{a^2}\right)^{\mu+1} \right\}$	$\phi(w) = -\frac{2\pi G \rho_0 a}{\Gamma(\mu+1)} \frac{\Gamma(\mu+1)}{\Gamma(\mu+1/2)} \times F\left(\frac{1}{2}, \mu - \frac{1}{2}, 1; \frac{w^2}{a^2}\right)$ $\pi \frac{\Gamma(\mu+1)}{\Gamma(\mu+1/2)} \frac{w}{a} \Gamma\left(\frac{1}{2}, \frac{1}{2} - \mu; \frac{w^2}{a^2}\right)$	$\frac{j}{j_0} = 1 - (1 - \varepsilon)^{2\mu}$ ($\rho_s \text{ const.}$)
$(1 - \frac{w^2}{a^2})^{1/2}$	$\frac{2}{3} \left\{ 1 - \left(1 - \frac{w^2}{a^2}\right)^{3/2} \right\}$	$\frac{\pi w}{2a} \left(1 - \frac{w^2}{a^2}\right)$ $\left(\frac{a}{w}\right)^{-1} \text{sn}^{-1}\left(\frac{w}{a}\right) - \sqrt{1 - \left(\frac{w}{a}\right)^2} \quad (w \rightarrow a)$	$\frac{j}{j_0} = 1 - (1 - \varepsilon)^{3/2}$
$e^{-w/a}$	$1 - e^{-w/a}$	$\sqrt{\pi} \frac{w}{a} e^{-w/2a}$ $\times \left\{ I_0\left(\frac{w^2}{2a^2}\right) - I_1\left(\frac{w^2}{2a^2}\right) \right\}$	$-\ln(1 - \varepsilon)$
$e^{-w/a}$	$2 \left\{ 1 - \left(1 + \frac{w}{a}\right) e^{-w/a} \right\}$	$2x \left\{ I_0(x) K_0(x) - I_1(x) K_1(x) \right\}$ $x = w/2a$	$j = 1 - \left\{ 1 + \left(\frac{1}{2x}\right)^2 \right\} e^{-4/x}$
$\frac{a}{w} e^{-w/a}$	$2 \left(1 - e^{-w/a}\right)$	$I_0(x) K_1(x) - I_1(x) K_0(x)$ $x = w/2a$	$j = \ln(1 - \varepsilon)^2$
$\frac{1}{1 + \frac{w^2}{a^2}}^{\mu+1}$ ($\mu > \frac{1}{2}$)	$\frac{1}{\mu} \left\{ 1 - \left(1 + \frac{w^2}{a^2}\right)^{-\mu} \right\}$ $\ln\left(1 + \frac{w^2}{a^2}\right)$ ($\mu=0$)	$\sqrt{\pi} \frac{\Gamma(\mu+1/2)}{\Gamma(\mu+1)} \left(1 + \frac{w^2}{a^2}\right)^{-1/2} \frac{w}{a}$ $\times F\left(\frac{1}{2}, \frac{1}{2} - \mu; 2; \frac{w^2}{a^2 + w^2}\right)$	$(1 - \varepsilon)^{-\mu} - 1$
$\frac{1}{1 + \frac{w^2}{a^2}}^{1/2}$	$2 \left\{ \sqrt{1 + \frac{w^2}{a^2}} - 1 \right\}$	$2 \frac{\sqrt{1+x^2} - 1}{x \sqrt{1+x^2}} \quad (x = w/a)$	MF: $\frac{j}{j_0} = \varepsilon \left(\frac{1+\varepsilon}{1-\varepsilon}\right)^{1/2}$
$\frac{1}{1 + \frac{w^2}{a^2}}^{1/2}$	$2 \left\{ 1 - \frac{1}{(1+x^2)^{1/2}} \right\}$ ($x = w/a$)	$\frac{2x}{(1+x^2)^{1/2}}$	$\frac{j}{j_0} = 2\varepsilon \frac{1-\varepsilon/\varepsilon}{(1-\varepsilon)^{1/2}}$

数値計算法

3D Resistive MHD 多層格子法数値コード

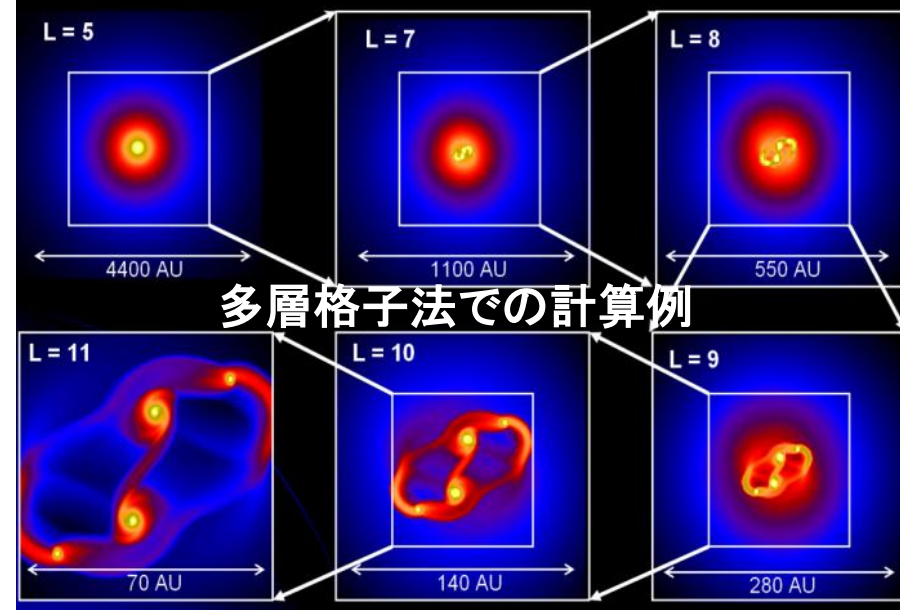
多層格子法とは、

- 異なるサイズのグリッドを入れ子状に配置
- 必要な場所に、必要な解像度：広範なスケールを計算可

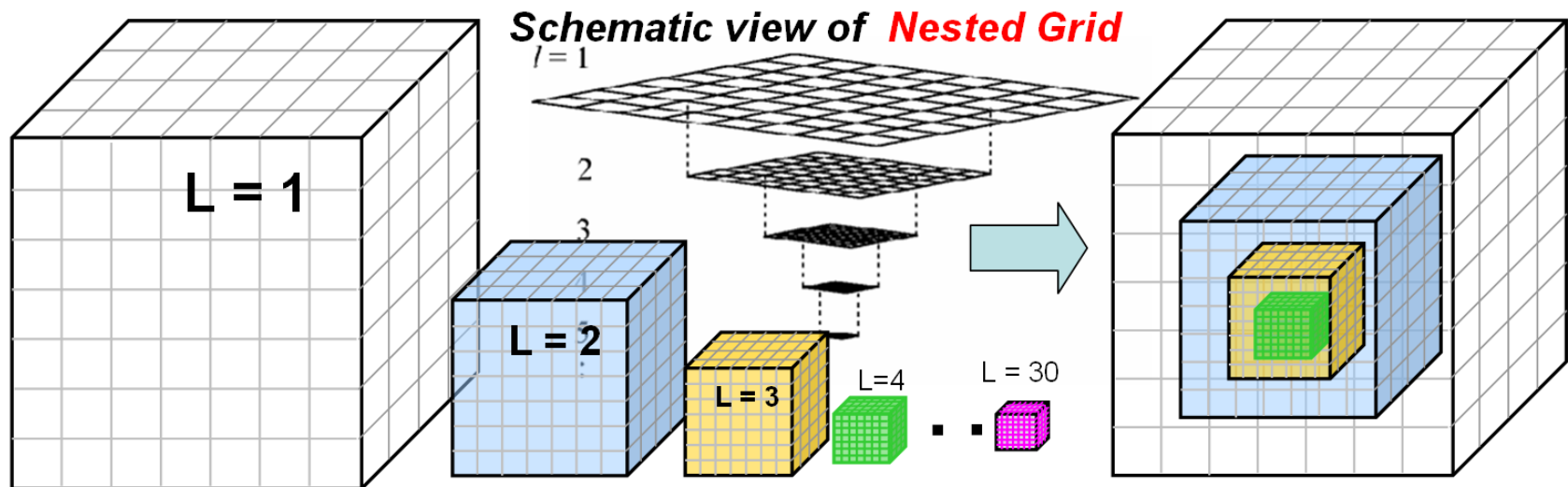
分子雲コアと原始星の両方を分解

- 空間10桁 (10^{14} km \sim 10 4 km), パーセク \sim 太陽半径まで
- 密度コントラスト20桁 (10^9 m $^{-3}$ \sim 10 29 m $^{-3}$)

流体: Resistive MHD 方程式 + 自己重力



同時刻、異なる空間スケール



Collapse of Magnetized Core

Before the Formation of **First Core**

Simple Self-Similar Collapse

Larger Scale

Inner Region

L0

L2



101

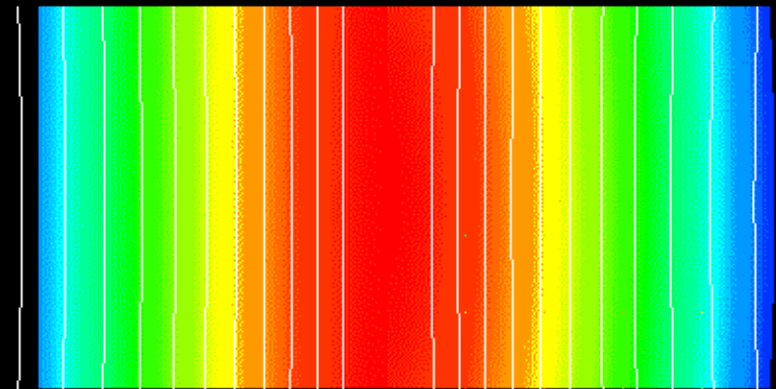
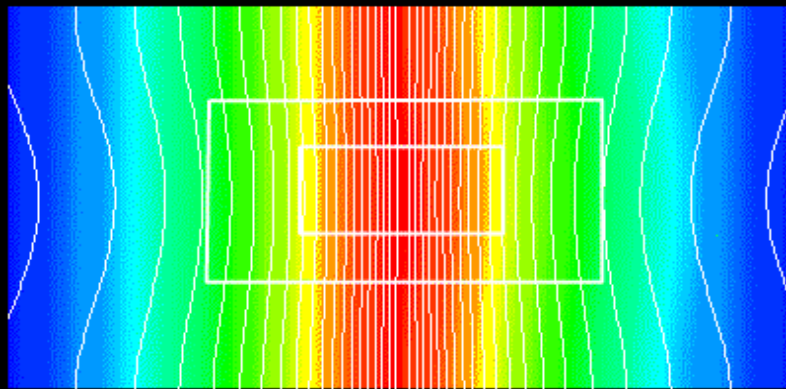
101

Z

Density

Z

Density



Omega

Omega



Tomisaka 2000, ApJ **578**, L41. See also Basu, Fiedler,

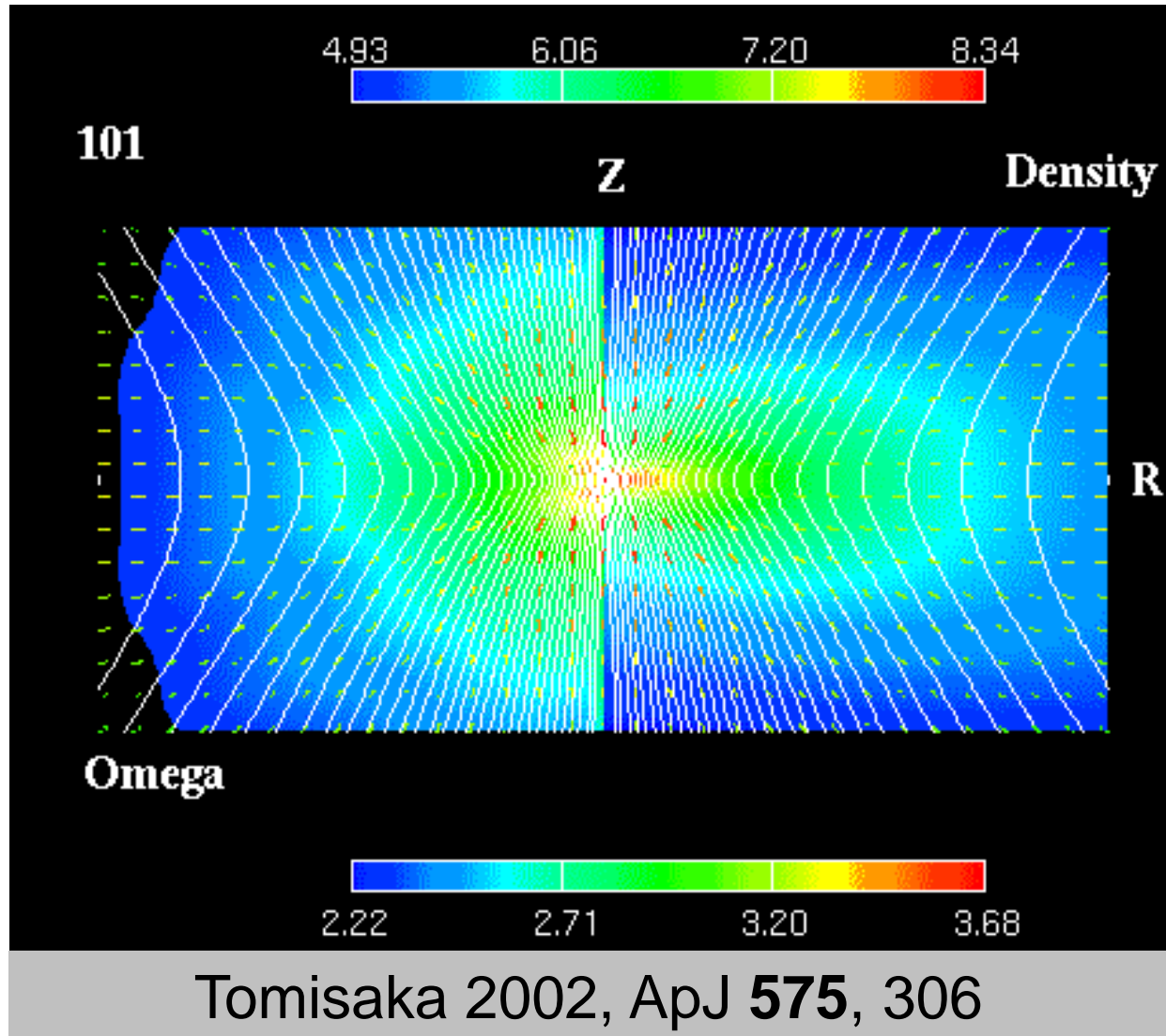
Onset of Outflow

After the
Formation of **First**
Core (2D calc.)

Rotation of
magnetic field lines



Onset of outflows



First Core形成の役割

その寿命は 10^3 yr 程度しかないが,...

重要

1. 円盤状構造の形成

→ 重力的分裂と連星系形成へ

2. MHD outflow の駆動

→ 角運動量の放出 ($\times 10^{-4}$)

First Coreの観測的発見

Chen et al. (2010) ApJ **715**, 1344

では、第2収縮以後は？

非理想MHDの効果

Weakly Ionized Gas

– Low density...

Ambipolar Diffusion

– Intermediate...

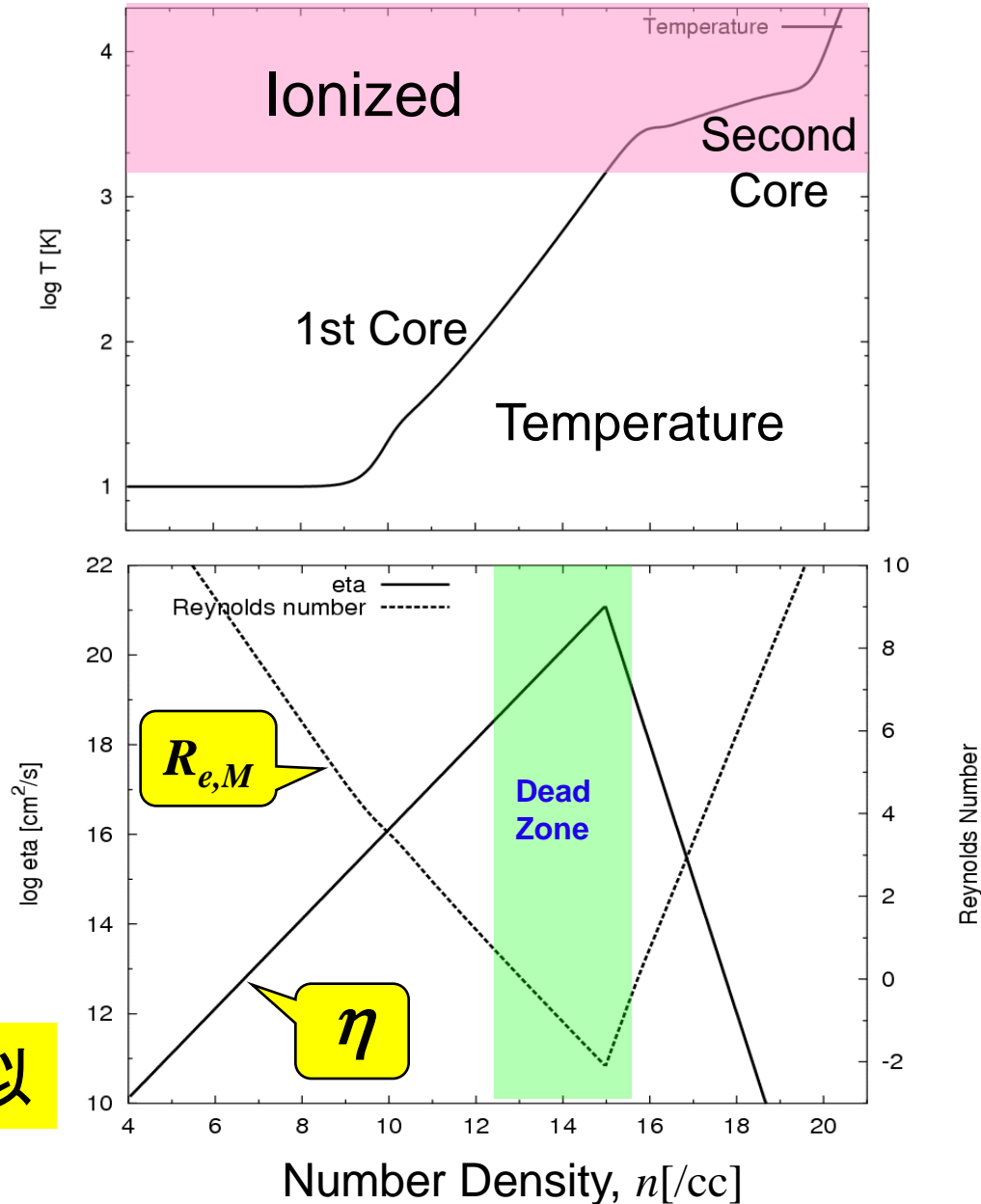
Hall Current Effect

– High density...

Ohmic Dissipation

e.g., *Nakano, Mouchouviats, Wardle, etc.*

太陽彩層での物理との類似



第一段階: **Outflow** driven from the **first core**

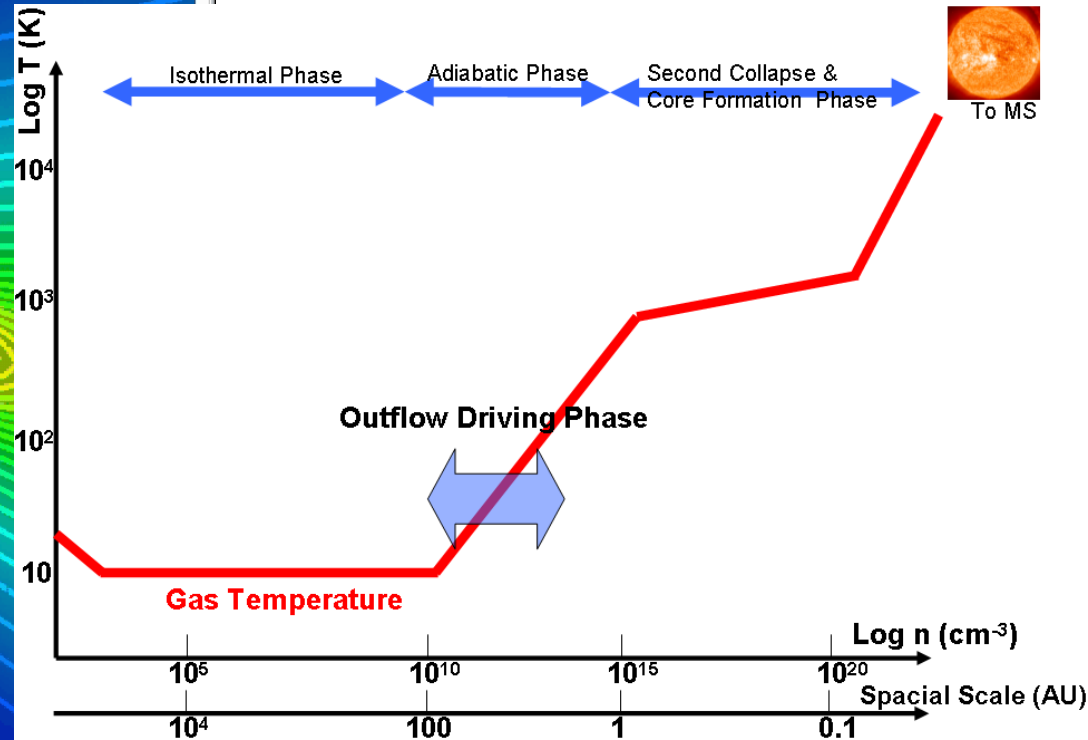
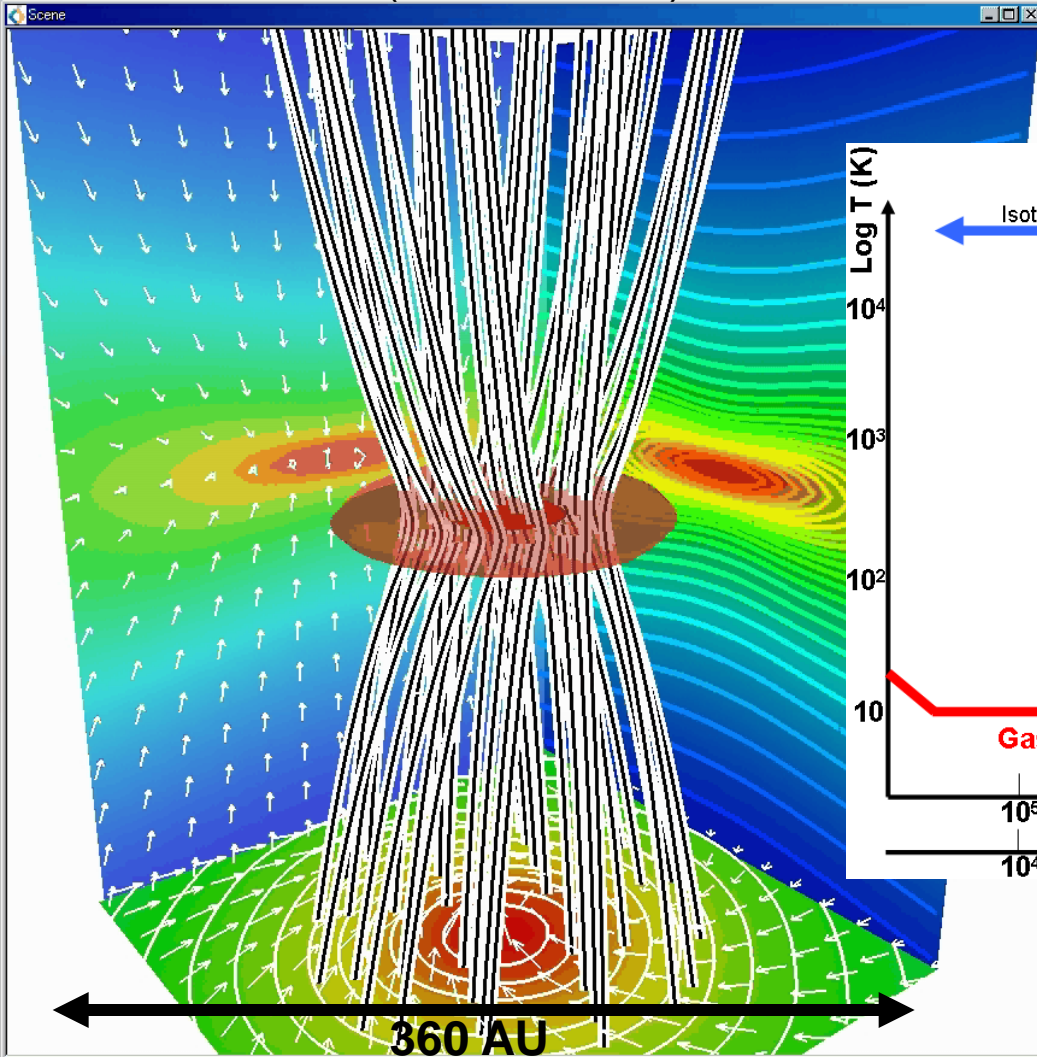
The evolution of the Outflow around the first core

➤ This animation start after the first core is formed at $n \sim 10^{10} \text{ cm}^{-3}$

Model for
 $(\alpha, \omega) = 1, 0.3$

Grid level $L=12$ (Side on view)

Grid level $L=12$ (Top on view)



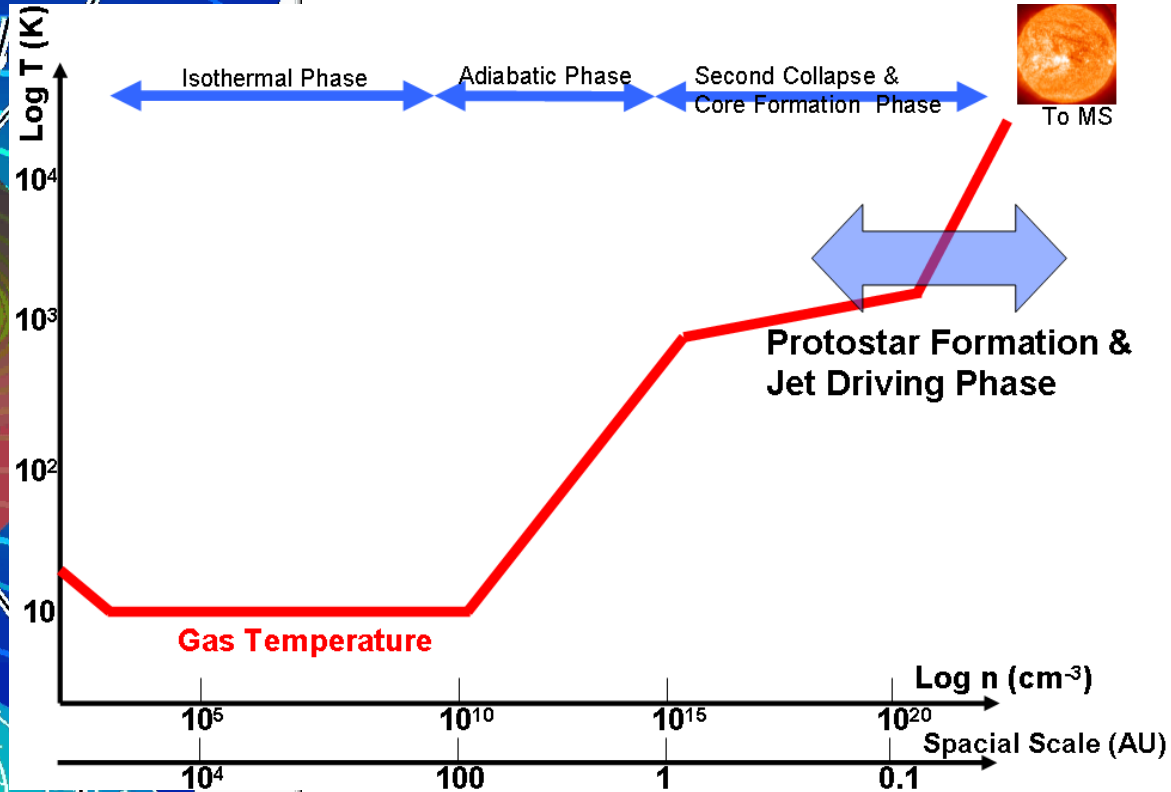
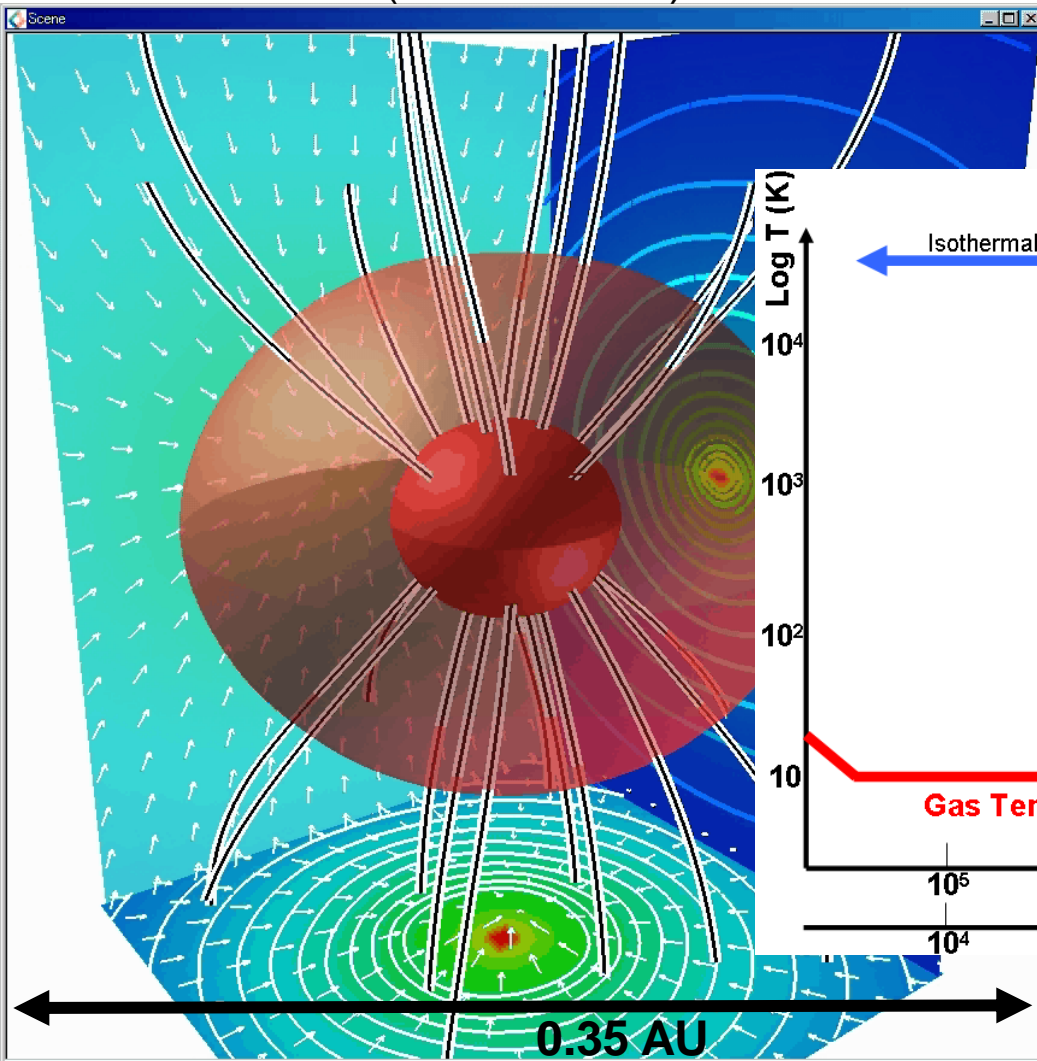
第2段階: Jet driven from the protostar

The evolution of the Jet around the protostar

➤ This animation start before the protostar is formed at $n \sim 10^{19} \text{ cm}^{-3}$

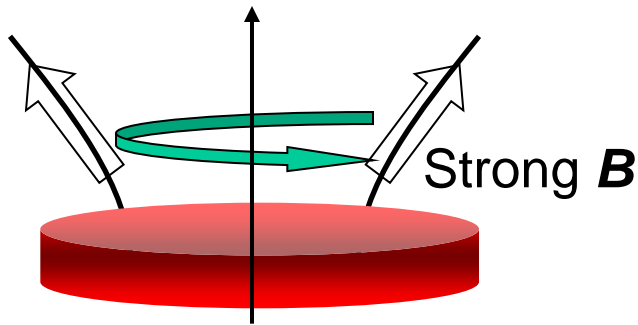
Model for
 $(\alpha, \omega) = 1, 0.003$

Grid level $L=21$ (Side on view)



駆動メカニズムの違い

Magnetocentrifugally driven Wind

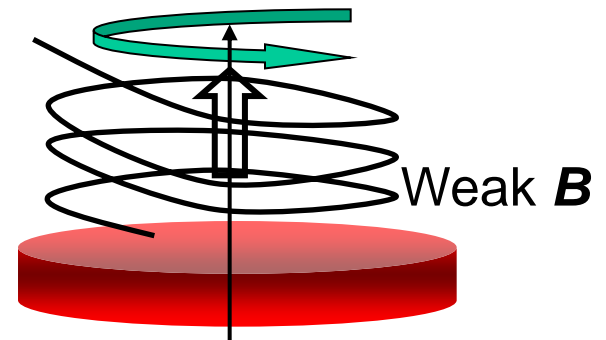


Wide Opening Angle

outflow around first core

$$B_r \approx B_z \approx B_\phi$$

Magnetic Pressure driven Wind



Narrow Opening Angle

jet around protostar

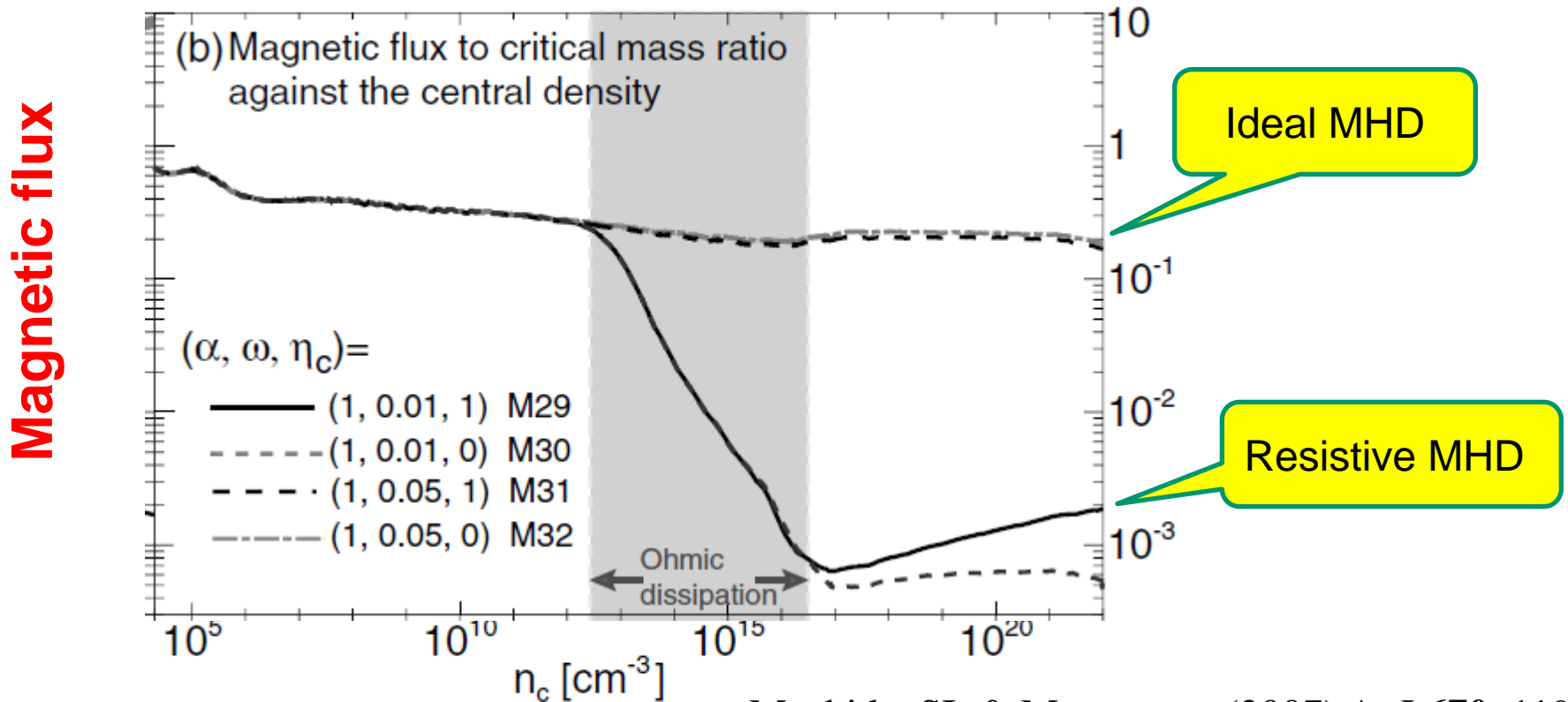
$$B_z \ll B_\phi$$

Good Collimation!

愚直な計算の賜物

Magnetic Flux Loss?

Magnetic flux largely removed from **First Core**
when $n = 10^{12} \sim 10^{16} \text{ cm}^{-3}$ $\rightarrow B = \text{kG}$ or less



Machida, SI, & Matsumoto (2007) ApJ **670**, 1198

原始星の磁場強度

●形成直後の原始星～キロ・ガウス

Machida, SI, & Matsumoto (2007) ApJ **670**, 1198

その後, 林フェイズの対流で外に放出されるはず

←“Turbulent Diffusion”... cf. Santos-Lima+ 2010

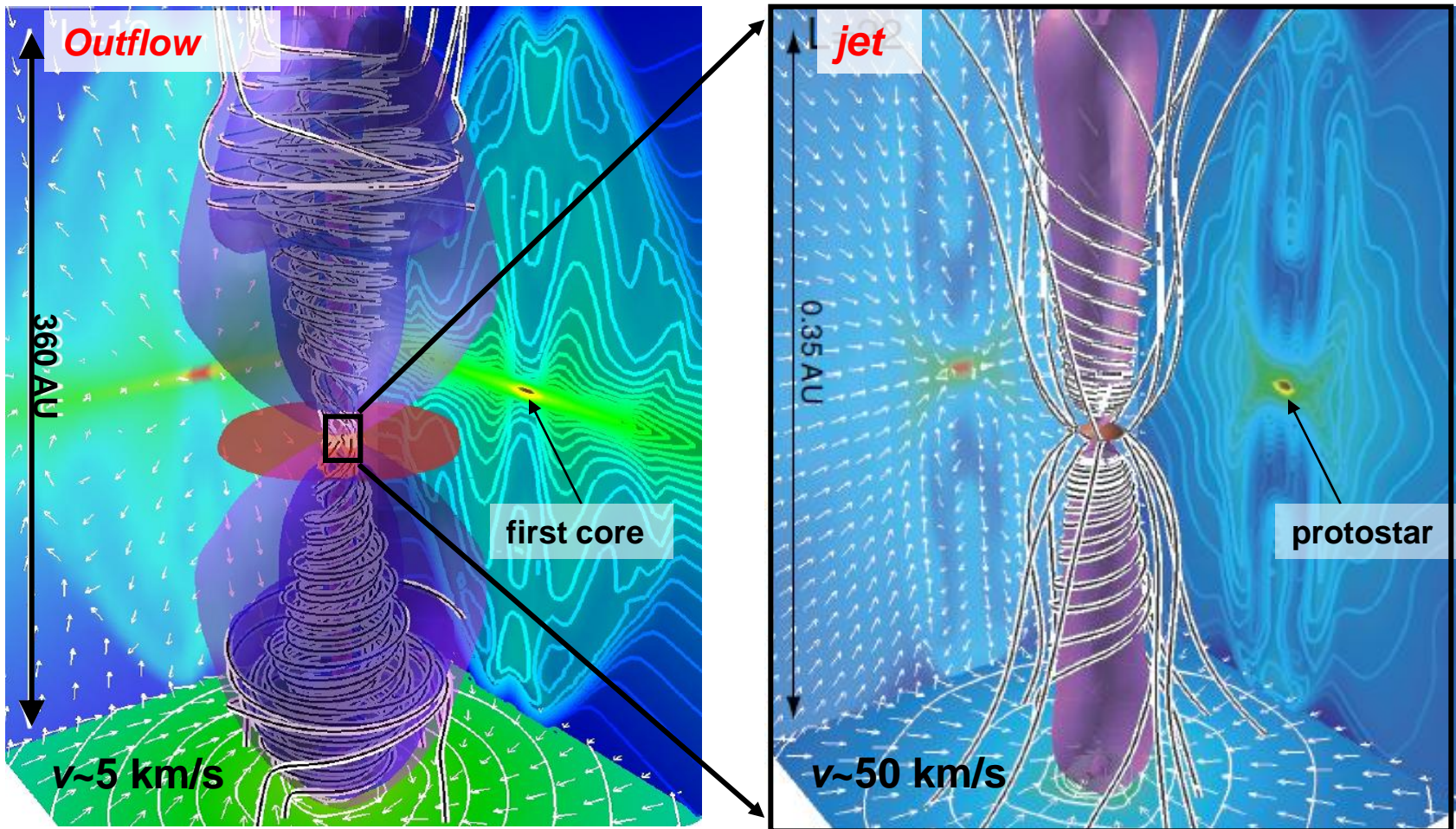
→磁場の強さは進化とともに減少するはず
(kG→G)

●T-Tauri型星の観測

Dipole等の低次成分はkG弱程度

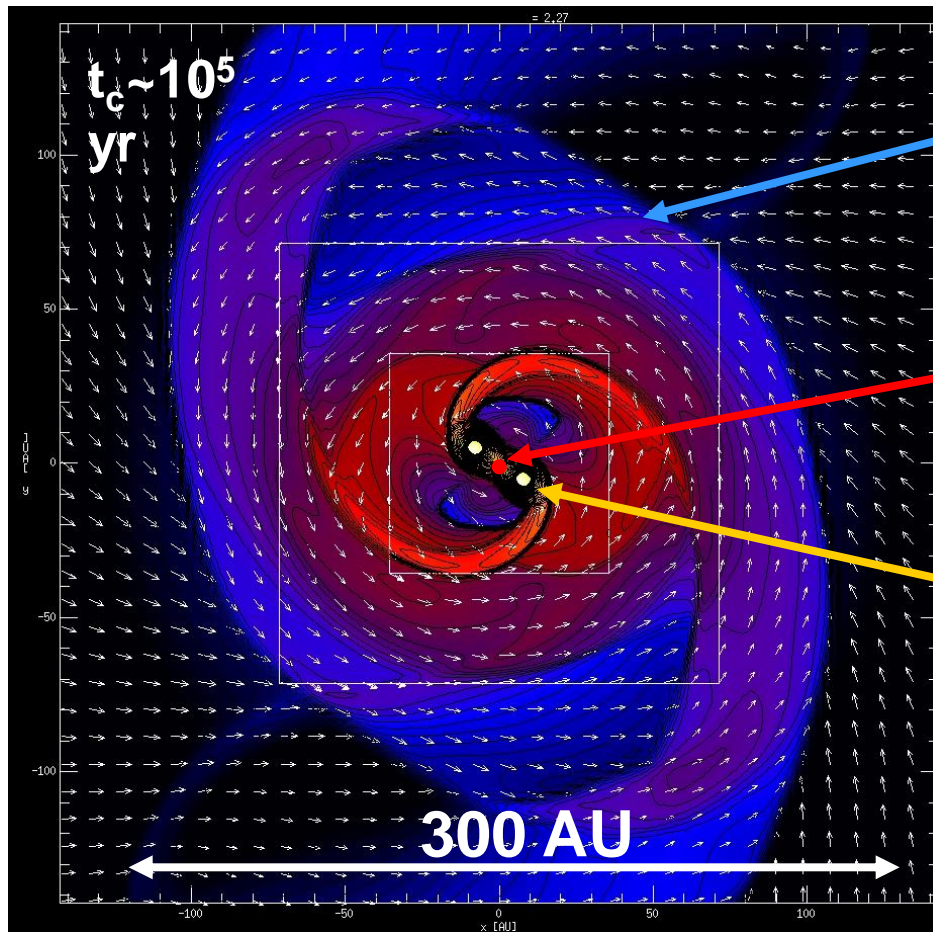
主系列星の初期磁場は無限小ではない

原始星形成期の理解



星形成過程は惑星形成の舞台を決める！

Formation of Planetary Mass Companions in Protoplanetary Disk



Protoplanetary Disk

Protostar

➤ $\sim 0.1 M_{\text{sun}}$

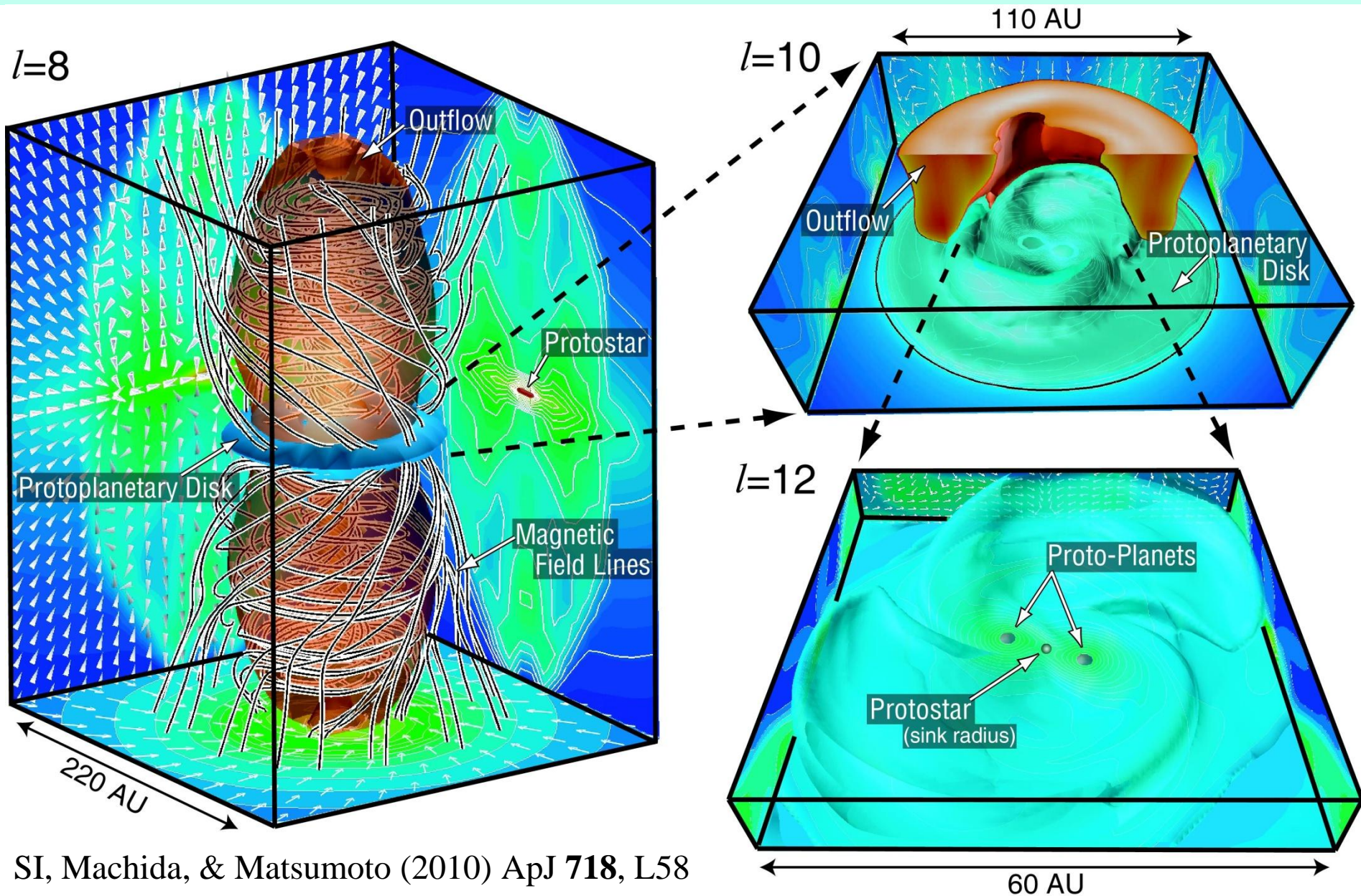
Protoplanet

➤ $M \sim 8 M_{\text{Jup}}$

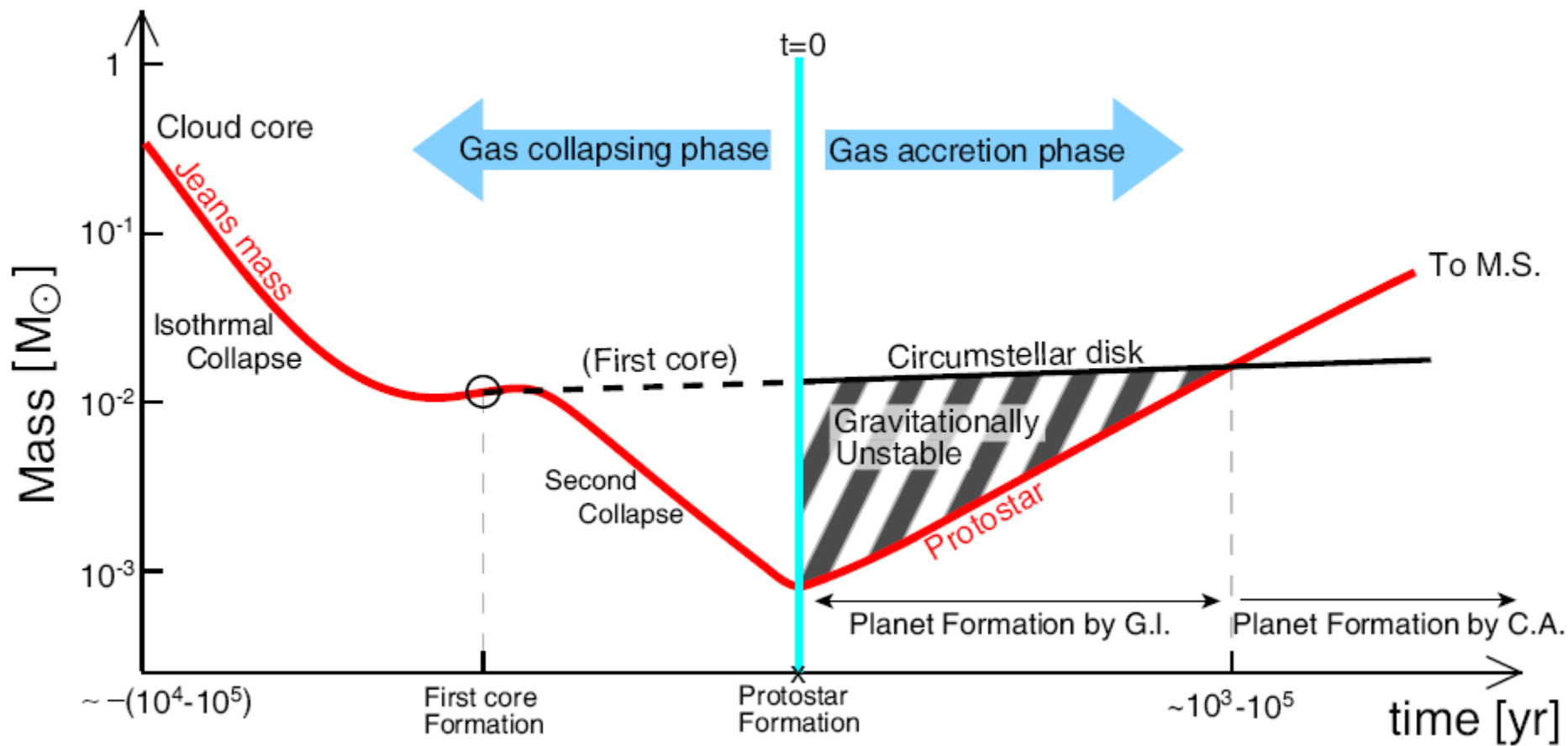
➤ $R_{\text{sep}} \sim 10\text{-}20 \text{ AU}$

Machida, SI, Matsumoto (2009)

Resistive MHD Calc. 分子雲コアから惑星へ



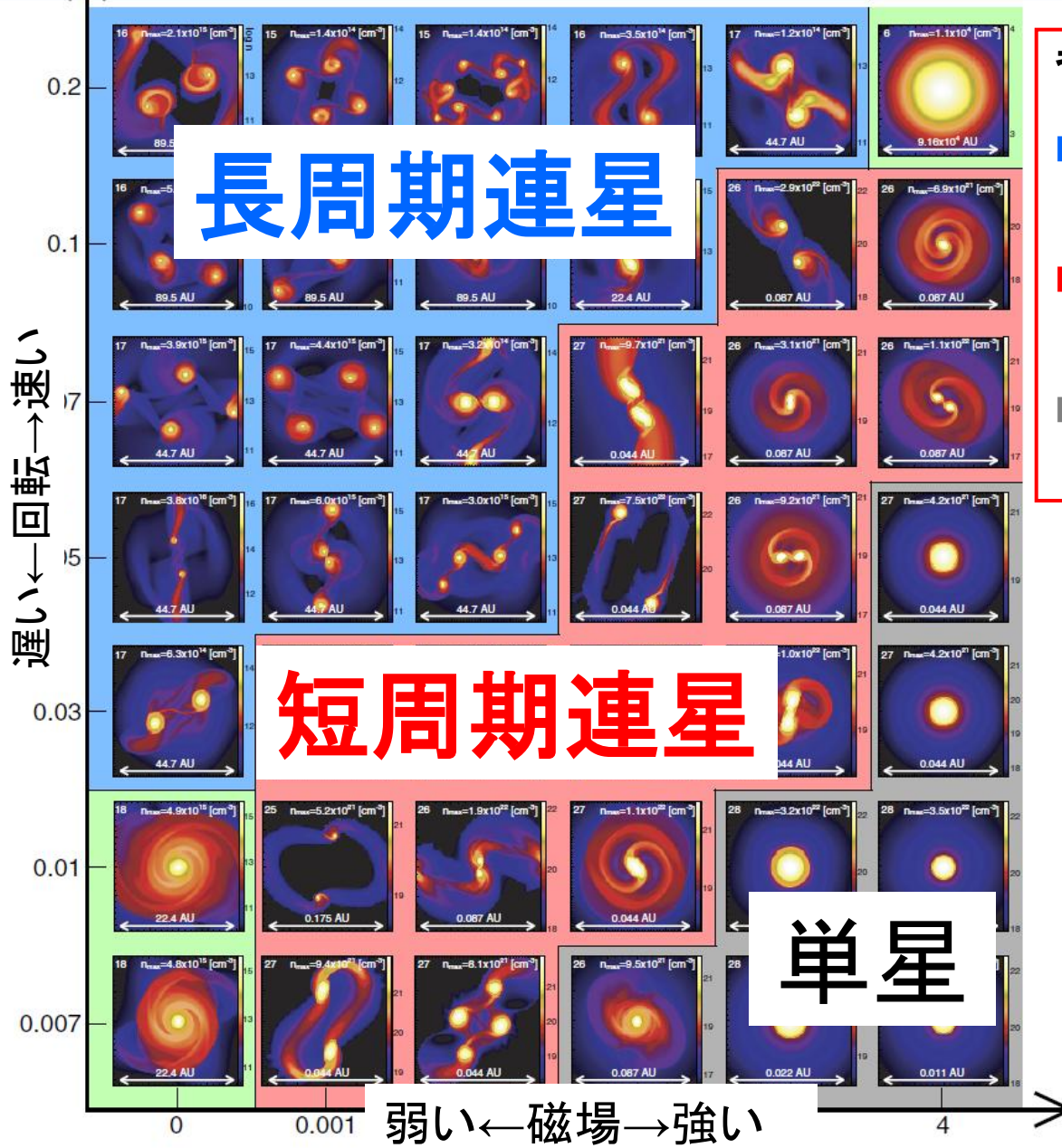
Formation of Planetary Mass Companions in Protoplanetary Disk



SI, Machida, & Matsumoto (2010) ApJ 718, L58

ガス収縮中の分裂と連星形成

Machida, Tomisaka, Matsumoto & Si
(2008) ApJ 677, 327



長周期連星

短周期連星

単星

背景の色

- 青:ファーストコア段階で分裂
wide binary ($r_{\text{sep}} > 1 \text{ AU}$)
- 赤:第二収縮期以降に分裂,
Close binary ($r_{\text{sep}} < 1 \text{ AU}$)
- 灰色:分裂無し
single star

- 磁場: 分裂を抑制
- 回転: 分裂を促進
- $E_{\text{mag}} / E_{\text{rot}}$ が唯一の
パラメータ

まとめ

- 原始星の形成過程

分子雲コアの第1収縮

→ 第1コア形成とOutflowの駆動

角運動量問題の解決

→ 第2収縮と磁場の散逸

磁束問題の解決

→ 第2コア(原始星)の形成とジェット駆動

- 第1コアが原始惑星系円盤の前駆体に！

円盤形成時は中心星に比べて重い→

渦状腕発生や重力分裂と伴星形成

今後の課題

- 円盤の長期進化と惑星形成

- 大質量星や星団の形成(星形成率の決定)

Part 2

Formation of Molecular Clouds

銀河内星間空間の環境

- Dynamical 3-Phase Medium

Cox & Smith 1974, McKee & Ostriker 1977

- 銀河系での超新星爆発率... 約 10^2 年に一発

- Expansion Time... 10^6 年

- Expansion Radius... 100pc

$$10^6 \text{年} \div 10^2 \text{年} \times (100 \text{pc})^3$$

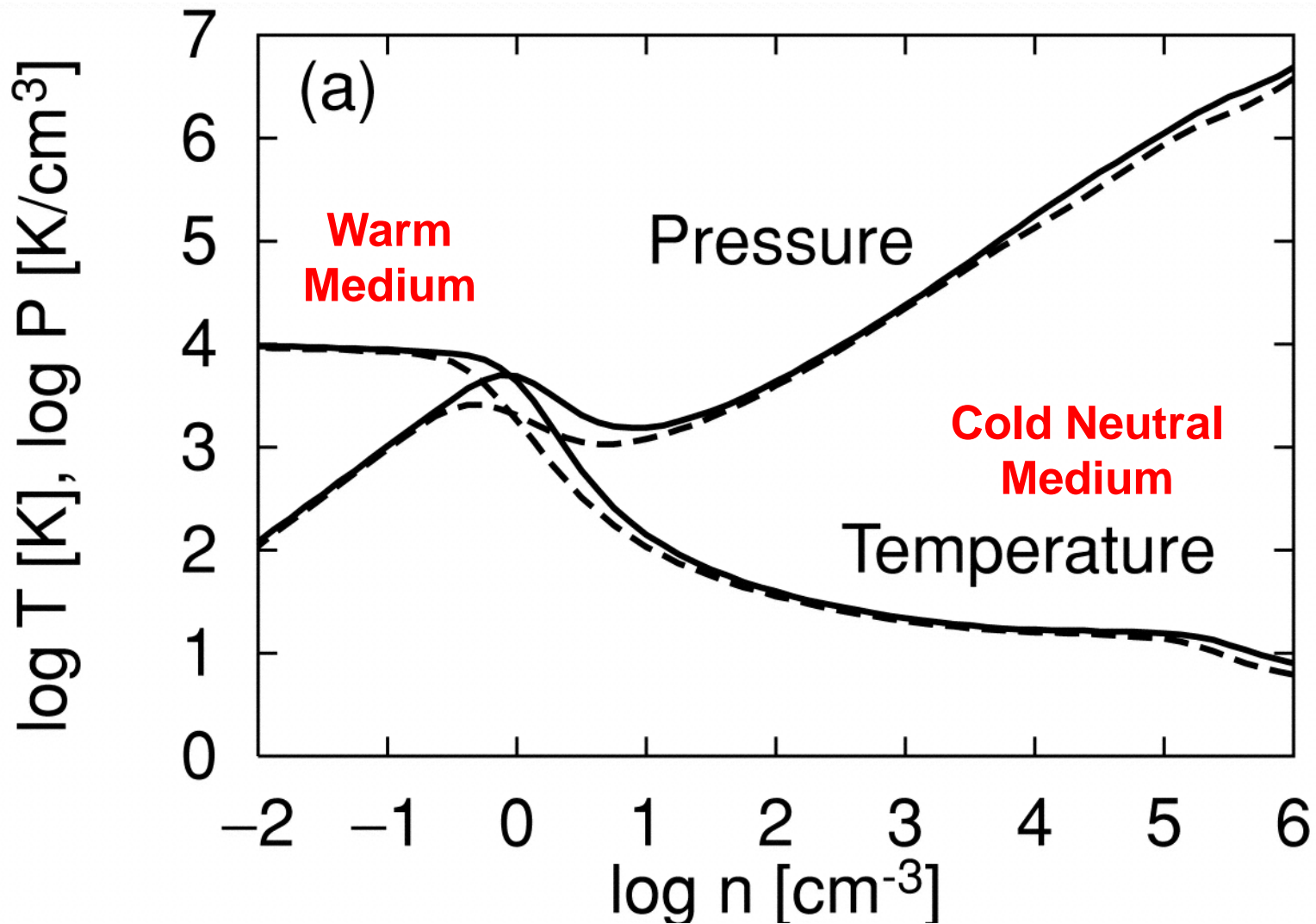
$$= 10^{10} \text{pc}^3 \sim \text{銀河円盤の体積}$$

- ◎ 星間ガスの動的時間尺度 $\sim 10^6 \text{yr}$

- ◀ 銀河円盤の密度波の時間尺度 $\sim 10^8 \text{yr}$

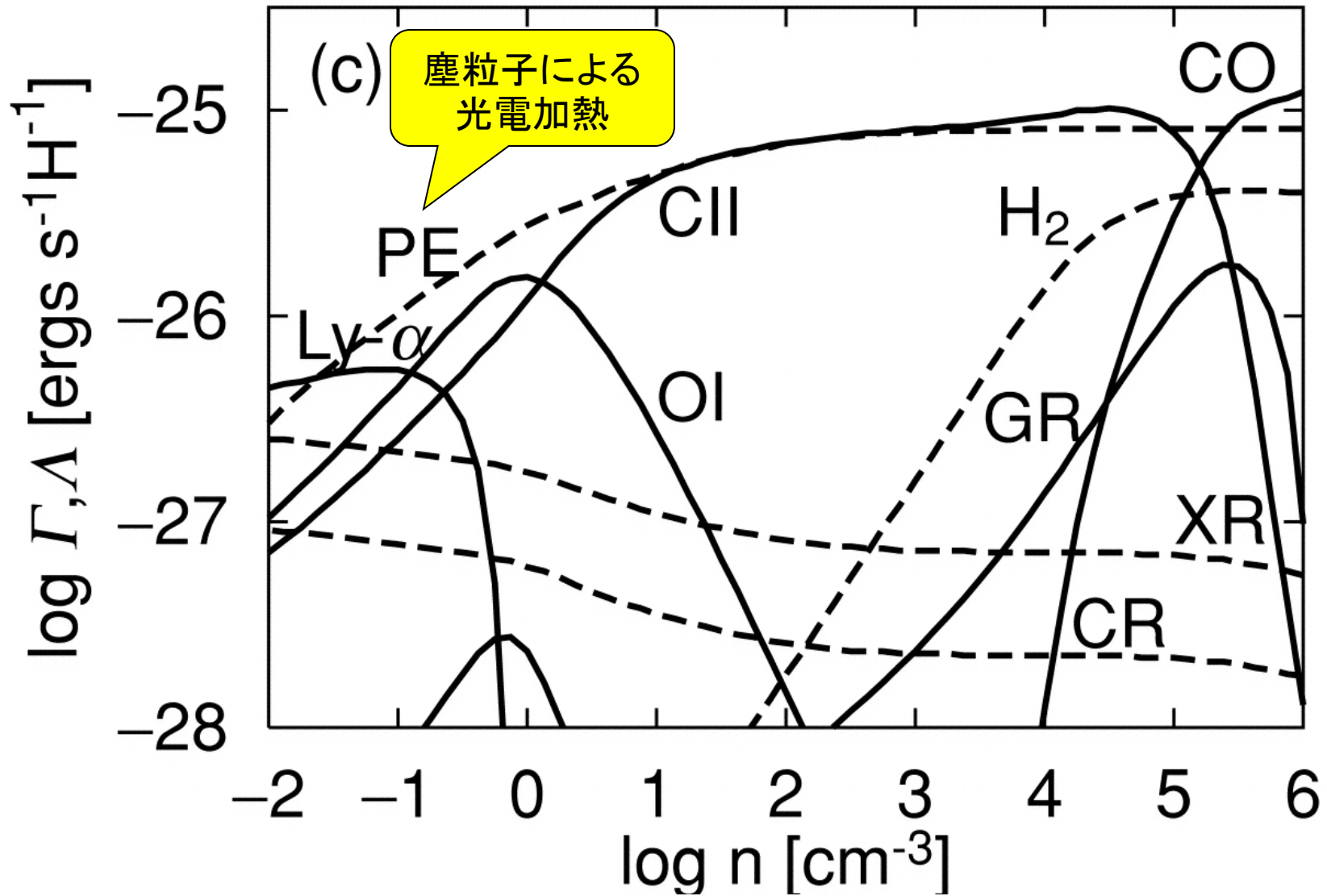
※ 星間空間は非常に動的な環境

輻射平衡狀態



實線：柱密度 10^{19} cm^{-2} 、破線：柱密度 10^{20} cm^{-2}

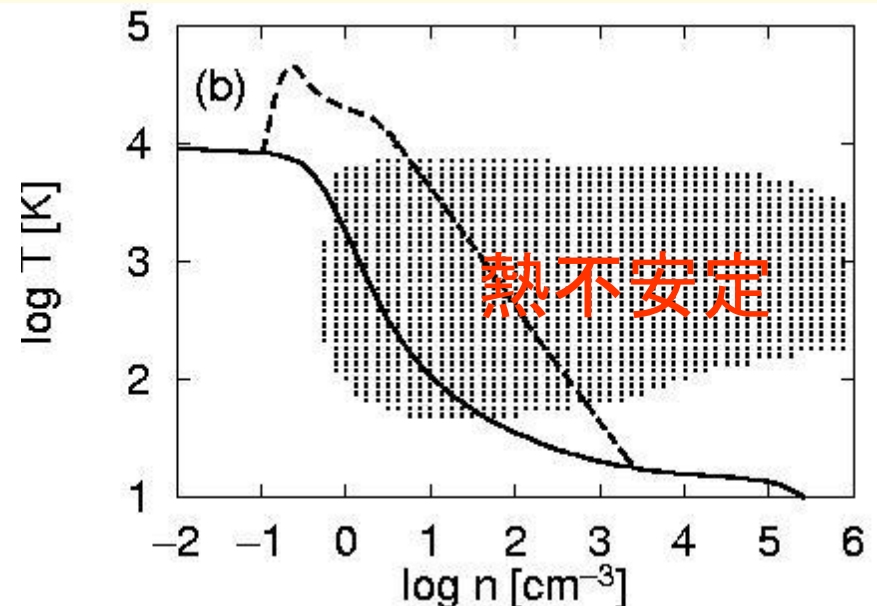
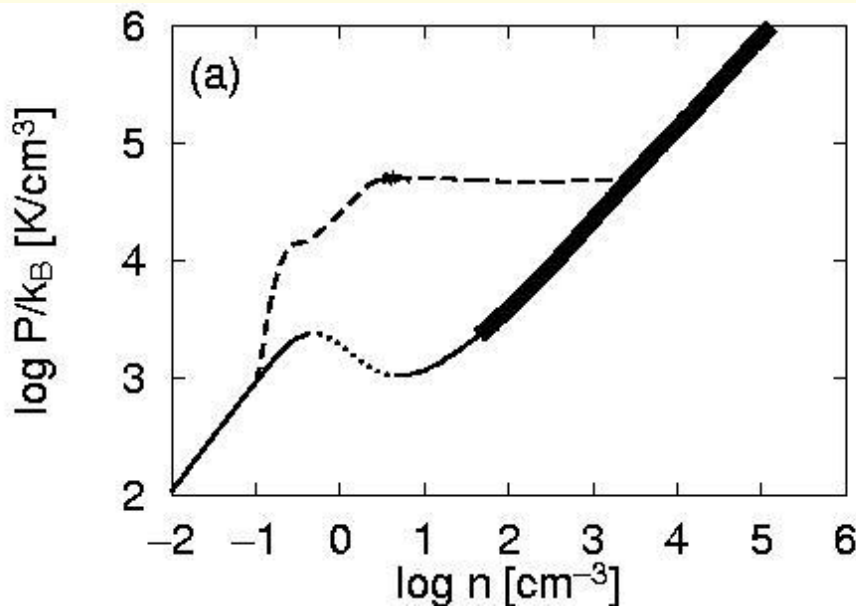
輻射加熱(破線)と冷却(実線)



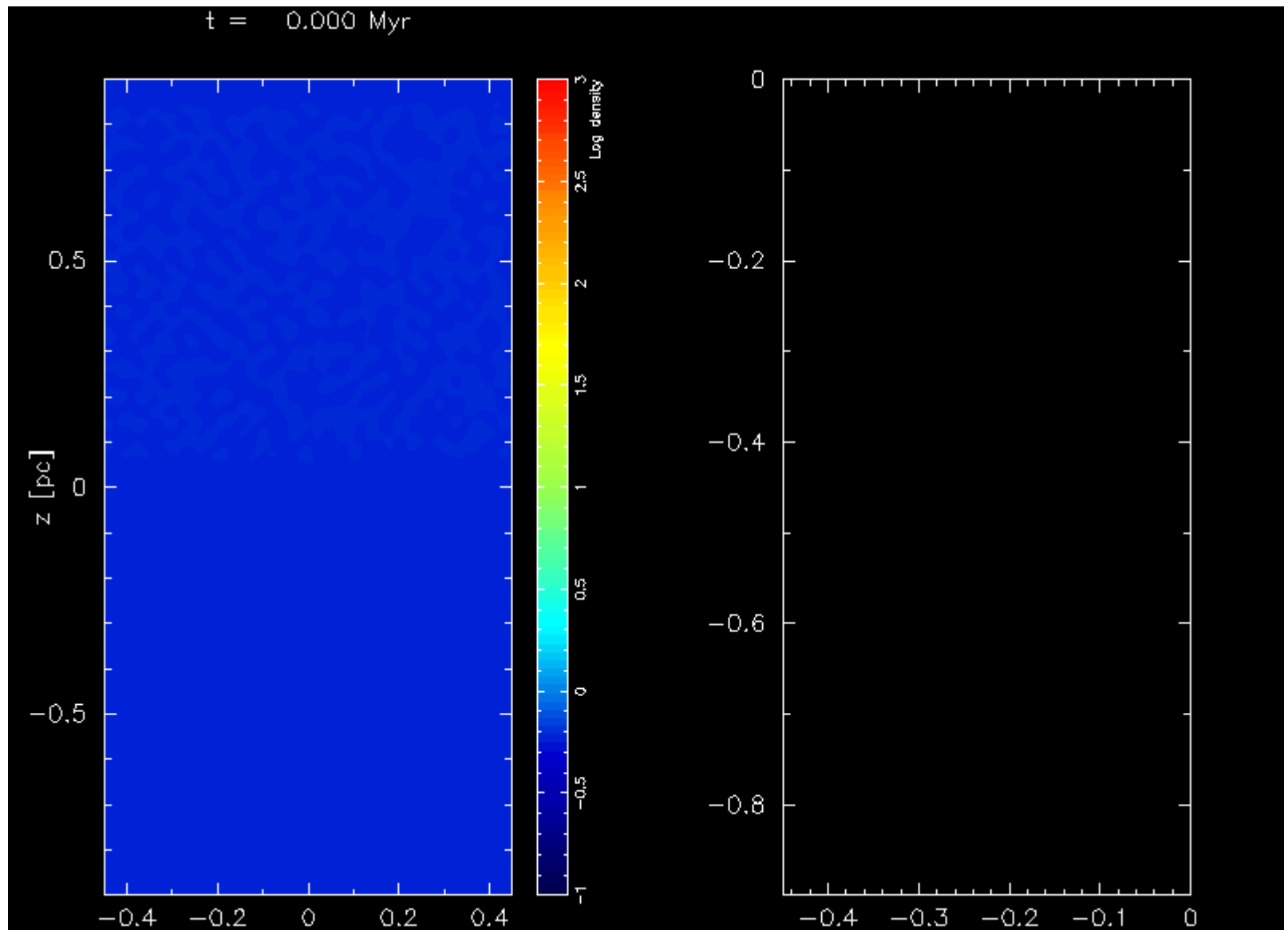
冷却収縮した層の進化トラック

- n-P diagram
ほぼ **isobaric**

- n-T diagram
必ず不安定な領域を通る

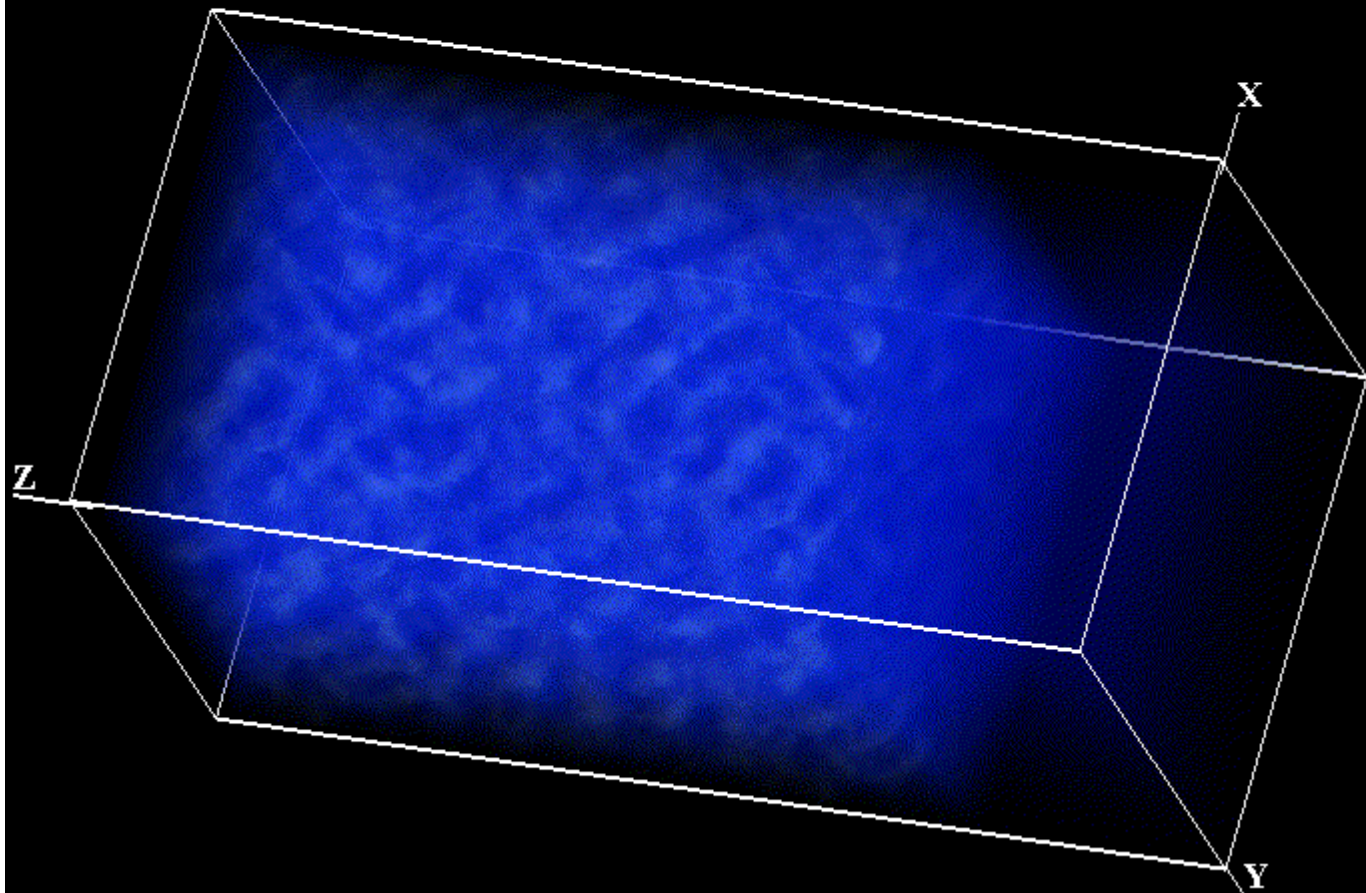


WNM($\sim 10^4\text{K}$)への衝撃波伝播



WNM($\sim 10^4\text{K}$)への衝撃波伝播

WNM Swept-Up by 14.4km/s Shock (3D)
Koyama & Inutsuka 2002

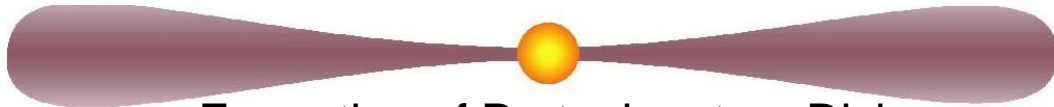


まとめに換えて

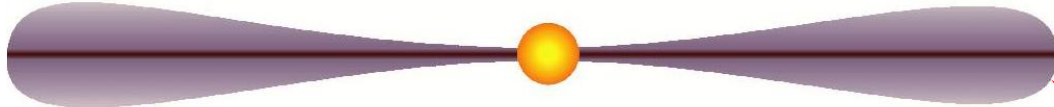
- これからも基礎方程式を愚直に解いて理論計算を進める
- 弟子達にもその姿勢を伝授する

Two Problems in Standard Model of Planet Formation

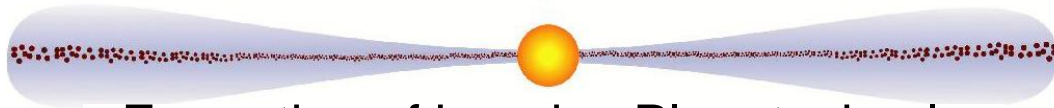
Formation of Protoplanetary Disk



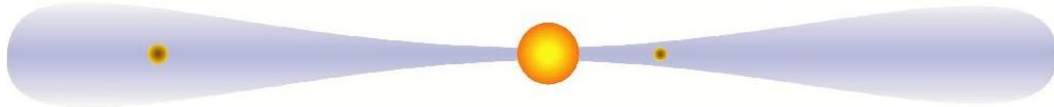
Sedimentation of Dust Grains onto Equatorial Plane



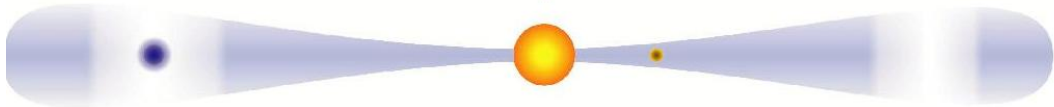
Formation of km-size Planetesimals



Coalescence of Planetesimals to Form Protoplanets



Gas-Capture of Massive Jovian Planets



Dispersal of Gas



Kelvin-Helmholz instability hinders dust sedimentation!

Gravitational interaction between planet and gas disk makes **planet migration** onto the central star!

Formation & Evolution of Discs

Further Evolution of Protostars

= Accretion of Gas from the envelope &
Gas Accretion through the Discs

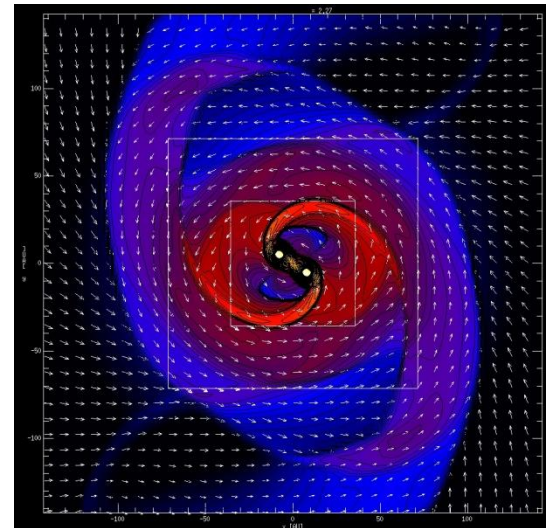
Early Phase

Rapid Gas Accretion due to
Gravitational Torque of
“ $m=2$ ” Spiral Mode

Later Phase

Slow Accretion due to Magnetorotational Instability

Velikhov 1959, Chandrasekhar 1961, Balbus & Hawley 1991



降着円盤の角運動量輸送

- 角運動量輸送 \Rightarrow 降着円盤の構造・進化
- 現在最も有力な機構
 - 磁気回転不安定性 \leftarrow 差動回転円盤 + 磁場
Velikhov 1959, Chandrasekhar 1961, Balbus & Hawley 1991
 - 非線形段階ではMHD乱流
 - 磁気応力による角運動量輸送

Std Model of Protoplanetary Disks

$$\Sigma_e(r) = 1.7 \times 10^3 f_\Sigma \left(\frac{r}{1\text{AU}} \right)^{-\frac{3}{2}} \frac{\text{g}}{\text{cm}^2}$$

$$T(r) = 280 \left(\frac{r}{1\text{AU}} \right)^{-\frac{1}{2}} \text{K}$$

$$C_s(r) \approx 10^5 \left(\frac{r}{1\text{AU}} \right)^{-\frac{1}{4}} \left(\frac{\mu}{2.34} \right)^{-\frac{1}{2}} \frac{\text{cm}}{\text{s}}$$

$$\rho(r, z) \approx 1.4 \times 10^{-9} f_\Sigma \left(\frac{r}{1\text{AU}} \right)^{-\frac{11}{4}} \left(\frac{M_*}{M_\odot} \right)^{\frac{1}{2}} \left(\frac{\mu}{2.34} \right)^{\frac{1}{2}} \text{g/cm}^3$$

$$B(r) \approx 1.9 f_\Sigma^{\frac{1}{2}} \left(\frac{r}{1\text{AU}} \right)^{-\frac{13}{8}} \left(\frac{\beta_c}{100} \right)^{-\frac{1}{2}} \text{G}, \quad \beta_c \equiv \left(\frac{2C_s^2}{v_A^2} \right)$$

Ionization Degree in PP Disks

neutral gas + ionized gas
+ **dust grains**

$$\zeta_{\text{CR}} = 10^{-17} \text{ s}^{-1}$$

cosmic ray ionization
 \Rightarrow resistivity

Classical Models:

Sano et al. 2000, ApJ **543**, 486

Glassgold et al. 2000, PPIV

Fromang et al. 2002, MN **329**, 18

Salmeron & Wardle 2003, MN **345**, 992

"**Dead Zone**" is the site of planet formation
in "**the standard model.**"

Sano, et al. 2000, ApJ **543**, 486

